

"HESIS



This is to certify that the

dissertation entitled

THE IDENTIFICATION OF MUTATIONS RESPONSIBLE FOR WAARDENBURG SYNDROME

presented by

ROBERT JAMES MORELL

has been accepted towards fulfillment of the requirements for

PhD degree in Zoology

Major professor

Date 7-9-93

MSU is an Affirmative Action/Equal Opportunity Institution

0-12771

LIBRARY Michigan State University

PLACE IN RETURN BOX to remove this checkout from your record. TO AVOID FINES return on or before date due.

DATE DUE	DATE DUE	DATE DUE
т. 19 95 - 1995 -		MARU 4 1007
FEB 1 5 1996		
NOS 24 1998		

MSU Is An Affirmative Action/Equal Opportunity Institution

THE IDENTIFICATION OF MUTATIONS RESPONSIBLE FOR WAARDENBURG SYNDROME

By

Robert James Morell

A DISSERTATION

Submitted to
Michigan State University
in partial fulfillment of the requirements
for the degree of

DOCTOR OF PHILOSOPHY

Department of Zoology

1993

ABSTRACT

THE IDENTIFICATION OF MUTATIONS RESPONSIBLE FOR WAARDENBURG SYNDROME

By

Robert James Morell

Waardenburg syndrome (WS) is an autosomal dominant mutation originally characterized by congenital deafness, dystopia canthorum, heterochromia irides, poliosis, broad nasal root, and synophrys. Since the original description of the syndrome, other clinical characteristics have been reported in the literature, including aganglionic megacolon, upper-limb deformities, spina bifida, leukoderma, and meningomyelocele. WS exhibits reduced penetrance and variable expressivity for all of the clinical features, even within families. On the basis of the segregation of discrete subsets of the clinical features within certain families, investigators have maintained that the syndrome is clinically heterogeneous, and have described at least four types of Waardenburg syndromes: WS1, WS2, WS3 and WS4. Whether the apparent clinical heterogeneity reflects an underlying genetic heterogeneity, or is an artifact of cosegregation of modifier genes within families, is a subject of dispute.

Some WS1 mutations have been mapped to chromosome 2q37, in a region of conserved syntenies between the murine and human genetic maps. The murine mutation Splotch (Sp) was hypothesized to be the homolog of the 2q37 WS1 mutations by virtue of its similar phenotype and location on the genetic map. Several alleles of Sp have been shown to be mutations of Pax-3. On this basis, mutations in human PAX3 were sought and identified in individuals with WS1, and are arguably the primary cause of the WS1 phenotype. The molecular events giving rise to WS are still far from understood since normal PAX3 function and regulation are not known.

We have characterized two mutations in PAX3 causing WS1. These mutations offer a better understanding of the molecular pathology of WS, and suggest that the WS phenotype arises as the result of haploinsufficiency of PAX3. We have also tested for linkage of WS mutations to PAX3 in several families and found evidence that WS is genetically, as well as clinically, heterogeneous.

ACKNOWLEDGEMENTS

I would like to thank Tom Friedman and Jim Asher for their patience, enthusiasm and many interesting discussions; Tom Barber, Jean Burnett, Peter Crawley, Sue Lootens, Lenny Robbins, Robin Steinman, Ellen Swanson, Mark Thompson, Lori Wallrath and Brian Wissink, for many pow-wows, both scientific and non-scientific; and Pat Venta and Jim Higgins, members of my committee, for helpful suggestions. All of the Waardenburg syndrome families described in this thesis were identified and characterized in whole or in part by Jim Asher.

I would especially like to thank John and Sue McRorie. Without their friendship and moral support I would have had neither the strength nor the desire to endure graduate school.

TABLE OF CONTENTS

List of Tables	vi
List of Figures	vii
Glossary and Symbols	vii.
INTRODUCTION	1
I CHAPTER ONE: Genetic linkage mapping of Waardenburg syndrome to chromosome 2q. A. Introduction B. Results 1. Linkage analysis of MSU4 2. Linkage analysis of MSU5 3. Linkage analysis of MSU6 4. Linkage analysis of UGM1 C. Discussion	5 9 9 13 17 23 28
II. CHAPTER TWO: Mutations in PAX3 associated with Waardenburg syndrome. A. Introduction B. Results C. Discussion	33 33 36 49
III. APPENDIX A: Materials and Methods 1. Evaluation of Subjects 2. Preparation of Genomic DNA 3. Southern Blots 4. PCR Amplifications 5. Genotyping for Dinucleotide Repeat Markers 6. SSCP Analysis 7. Sequencing 8. Linkage Analysis	59 59 60 61 62 63 65
IV. APPENDIX B: Additional Figures and Tables	67
V. APPENDIX C: Detection of Changes in Copy Number at Regions of Candidate Loci By Dot Blot Analysis	74
VI. APPENDIX D: Conventions of Nomenclature for Human Alleles Used in this Thesis	84
VII.APPENDIX E: Results of Linkage Analysis for Mi ^{OR} .	87
VIII LIST OF REFERENCES	90

LIST OF TABLES

Table	1	Phenotypes of Affected Members of Family MSU4	9
Table	2	MSU4 Linkage Results	12
Table	3	Phenotypes of Affected Members of Family MSU5	14
Table	4	MSU5 Linkage Results	17
Table	5	Phenotypes of Members of Family MSU6	18
Table	6	MSU6 Linkage Results	22
Table	7	Phenotypes of Affected Members of Family UGM1	23
Table	8	Comparisons of a/b Ratios Between Indonesians and Caucasians	25
Table	9	UGM1 Linkage Results	26
Table	10	Phenotypes of WS Subjects	38
Table	A1	Waardenburg Consortium Criteria	59
Table	A 2	PCR and Sequencing Primers	66
Table	В1	MSU4 Linkage Data File	67
Table	B2	MSU5 Linkage Data File	68
Table	В3	MSU6 Linkage Data File	69
Table	В4	UGM1 Linkage Data File	70
Table	C1	Ratios of PAX3 exon Copy Numbers to Other Loci	77
Table	C2	Ratios of Non-PAX3 Loci Comparisons	78
Table	E1	Linkage results for $Mi^{OR}/+ \times +/+ \dots$	88

LIST OF FIGURES

Figure	1	MSU4 Pedigree	10
Figure	2	MSU5 Pedigree	15
Figure	3	MSU6 Pedigree	19
Figure	4	UGM1 Pedigree	24
Figure	5	SSCP Analysis of PAX3 Exon 2 PCR Fragments in Affected Individuals	37
Figure	6	Sequence of Mutant PAX3 Allele Responsible for WS1 in Family MSU3	39
Figure	7	Confirmation of the Segregation of a Mutant Allele in Family MSU3	41
Figure	8	Sequence of the Mutant PAX3 Allele Segregating in UGM2	45
Figure	9	UGM2 Pedigree and Southern Blot Detection of a Mutant PAX3 Allele	47
Figure	10	Summary of all WS mutations in PAX3 published to date	51
Figure	В1	MSU4 PAX3 Gel	71
Figure	В2	MSU4 CD3D Gel	72
Figure	в3	MSU4 D11S35 Gel	73

SYMBOLS AND GLOSSARY

Aganglionic megacolon	=	Distension of the colon due to insufficient autonomic innervation and consequent difficulty in voiding. Also called Hirschsprung's disease.
Dystopia canthorum	=	Lateral displacement of the medial aspect of the canthi, or eye orbits, relative to the rest of the face.
Heterochromia iridis	=	Different colored sectors of same iris, or different color of two irides. May be hereditary as in Waardenburg syndrome or acquired by damage to sympathetic innervevation of eye.
Leukoderma	=	Depigmentation of skin. May be hereditary as in Waardenburg syndrome, or acquired by injury or infection as in <i>vitiligo</i> . Note that the latter term is erroneously used as a synonym in the medical literature.
PAX3	=	Human gene, mutant alleles of which are thought to be the primary cause of some cases of Waardenburg syndrome.
Pax-3	=	Murine gene. Splotch mutations are mutant alleles of Pax-3.
Poliosis	=	Strictly defined as whitening of the hair. In medical literature used as a synonym of congenital white forelock.
Ptosis	=	Strictly defined as "drooping" of any organ or body part. In medical literature means the drooping of upper eyelid, usually resulting from defects in sympathetic innervation to eye.
Sensorineural deafness	=	Deafness in reference to the sensory nerve, as opposed to deafness due to defects in mechanical transduction.
Splotch	=	Murine homolog of Waardenburg syndrome type 1. Alleles include: Sp , Sp^{2H} , Sp^{r} , Sp^{d} .
Synophrys	=	Confluent eyebrows.
ws	=	Waardenburg syndrome. At least four clinical subtypes described in the literature, abbreviated WS1, WS2, WS3 and WS4.

INTRODUCTION

The association of deafness with abnormal pigmentation in domesticated animals has long been known. Darwin [17], for instance, used the example of deafness and blue eyes in cats for general discussions on the co-inheritance of traits. And the prevalence of deafness in Dalmatian dogs and white minks was generally accepted long before it was scientifically confirmed [13,23]. Yet, except for isolated reports (for review see Fraser [23]), the phenomenon went largely unrecognized in humans until Waardenburg's 1951 paper [58].

Waardenburg described a form of deafness that cosegregated with pigmentary and facial abnormalities in 16 families. After first encountering a deaf patient who showed pronounced dystopia canthorum, or the lateral displacement of the lachrimael punctae relative to the rest of the face, he conducted an extensive survey of five Dutch schools for the deaf to find others with a similar phenotype. He realized that pigmentary anomalies were also prevalent among deaf children with dystopia canthorum, and he therefore defined the syndrome as comprising six clinical characteristics and estimated the penetrance for each by the incidence among affected members of the families, excluding the probands. The clinical manifestations were: 1) dystopia canthorum (99%); 2) broad nasal root (78%); 3) synophrys or confluent eyebrows (45%); 4) poliosis or white forelock (17%); 5) heterochromia iridum or differently colored irides

(irides either totally mismatched or a single iris containing differently pigmented sectors) (25%); and 6) congenital deafness (20%). Many other, less frequent, attributes were described, and they will be discussed later. The phenotype segregated as an autosomal dominant, and was variable both within and between families. Extrapolating from his sample, he estimated that the syndrome accounted for 1.43% of the institutionalized deaf population, and the gene had a population frequency of 1/42,000 and a mutation rate of 1/270,000.

It is important to note that Waardenburg was initially interested in the co-segregation of deafness with dystopia canthorum, thus his survey probably represents a biased sample. In particular, the high penetrance of dystopia canthorum led him to postulate that a single gene was responsible, although the reasoning may be tautological in that the syndrome was primarily defined in terms of the presence of this trait. However, among his 16 families, there were two in which dystopia canthorum did not manifest at all. One arguably represents a sporadic mutation due to the absence of any other affected members in the pedigree (family 4). The other (family 8) shows co-segregation of heterochromia irides with deafness in several members, and no other manifestations. Other researchers subsequently reported similar pedigrees and argued that they represented a distinct syndrome which they called Waardenburg syndrome

type 2 (WS2)[1,9,29], and which was defined as Waardenburg syndrome with the absence of dystopia canthorum.

A third type of Waardenburg syndrome (WS3) was proposed by researchers [26,51] who described patients manifesting severe musculo-skeletal abnormalities in addition to WS1-like features, and who otherwise resemble the patient first reported by Klein and described by Waardenburg [58]. All of these patients are severely affected and show no family history for any of the attributes. Therefore, they are probably the results of sporadic mutations, and most probably represent examples of contiguous gene syndromes. However, a family in which WS3 segregates as an autosomal dominant has recently been described [32,52].

Reports of Waardenburg syndrome type 1 (WS1) associated with aganglionic megacolon [6,23,25,41,44] seemed to merit a further subdivision as Waardenburg syndrome type 4 (WS4).

Arias[1] suggested yet another distinct clinical subtype to be known as "pseudo-Waardenburg" syndrome, the distinguishing feature of which is congenital, hereditary, unilateral ptosis.

The further subdividing of the phenotypes into clinical subtypes only emphasizes the challenge presented in Waardenburg's initial description of the syndrome in that the phenotype is highly variable in its expressivity and penetrance. It is important to note that each aspect of the phenotype has been reported in the literature to segregate as a single entity [58]. The obvious question raised, and

discussed by Asher and Friedman [4], is whether the primary cause is a single gene with pleiotropic effects, a single gene modified by various other loci, or several genes each of which can give rise to distinct clinical entities when mutated. The merits of each of these hypotheses will be discussed in the course of this thesis, but suffice to say at the outset that each hypothesis suggests a different strategy for identifying the molecular lesion responsible for Waardenburg syndrome. Further, any proposed mutation in a candidate gene would have to be compatible with a highly variable phenotype, and would have to address the question posed by Waardenburg as to what could account for the co-inheritance of a seemingly disparate constellation of attributes.

I. CHAPTER ONE: Genetic linkage mapping of Waardenburg syndrome to chromosome 2g.

A. Introduction

The hypothesis of a single gene exerting pleiotropic effects gained credence with the elucidation of neural crest cell development and the realization that all of the affected tissues in the syndrome are neural crest cell derivatives [6,35,41]. Accordingly, McKusick [44] proposed that the pleiotropy in WS can be explained by a single defect that affects neural crest cell migration and/or differentiation. This promised to make the task of finding the genetic cause easier since detecting genetic linkage to single locus disorders is significantly easier than detecting linkage in multi-locus disorders.

This optimism was somewhat mitigated by the fact that there were several genetically distinct mouse mutations that had been demonstrated to disrupt neural cell migration and/or differentiation and give rise to pigmentary abnormalities. These included: dominant spotting (Dom)[36], lethal-spotted (1s)[34]; various alleles at the microphthalmia locus (Mi) (summarized in Lyon and Searle[40]), piebald-lethal $(s^1)[61]$, Splotch (Sp)[5], and Steel (S1)[43]. Any one of these mouse mutations arguably could be the murine homolog of Waardenburg syndrome. Despite the number of candidate loci posed by mouse models for Waardenburg syndrome, the mouse mutations still suggested that a single

locus segregating in a family could account for the full extent of the phenotype in that family.

Asher and Friedman [4] favored Mi^{or}, Ph (Patch), s, and Sp as murine homologs because of the co-segregation of pigmentary anomalies and microphthalmia in Mi^{or}, aganglionic megacolon in s, and neural tube defects in Ph and Sp. All of these malformations had been reported in the literature in association with Waardenburg syndrome [45]. In particular, Waardenburg [58] described a case of microphthalmia and three instances of mild cleft face (furrowed forehead) in his original description of the syndrome.

Taking advantage of the conservation of syntenic groups between the human and murine genetic maps, Asher and Friedman predicted human chromosomal locations of 2q, 3p or 3q based on the locations of the predicted murine homologs on the murine map [48]. In recognition that the clinical heterogeneity of Waardenburg syndrome may reflect genetic heterogeneity, they suggested that linkage to markers in candidate regions be conducted in single pedigrees to avoid the false exclusion of regions due to the mixing of data from a genetically heterogeneous data set.

Exclusion of genetic linkage of WS1 to regions predicted by the Mi^{OT} [3] and S1 [22] models preceded the report by Ishikiriyama et al. [33] of a child exhibiting WS1 and having a de novo inversion (2) (q35q37.3)—a region predicted by Asher and Friedman on the basis of conserved syntenies surrounding the Sp locus. Foy et al.[22] and Asher

et al.[3] subsequently demonstrated genetic linkage of WS1 to markers on 2q, giving further support to the proposal that some WS1 mutations are human homologs of Sp.

In order to identify and clone the gene on 2q37 giving rise to WS1 in these families, a higher resolution genetic map was needed. In addition, the issue of possible genetic heterogeneity was still outstanding, especially given the fact that a negative LOD score in one family was reported by Foy et al.[22]. Both problems could be more readily addressed by pooling the data sets of the various laboratories that had done linkage analyses in Waardenburg syndrome families.

A consortium effort involving several laboratories, including ours at Michigan State University, demonstrated linkage heterogeneity among 44 kindreds segregating for Waardenburg syndrome, but failed to produce a genetic map with high enough resolution to make cloning efforts practical [20]. The closest linked marker, ALPP (Alkaline Phosphatase - Placental), mapped to approximately 7.6 cM away.

When the *Sp* phenotype was demonstrated to be the result of mutations in the gene *Pax-3* [18], efforts centered on investigating the homologous sequences in humans, HuP2 -- a lambda genomic clone which shows sequence similarities to exons 2, 3 and 4 of *Pax-3* [14]. Prior to the isolation of a cDNA of the human *Pax-3* homolog [32], a locus assignment of PAX3 was given for these three exons. Thus, the literature variously refers to the human gene as HuP2 or PAX3.

A dinucleotide repeat polymorphism was identified in a genomic clone containing the presumed exon 1 of the human PAX3 gene, and was shown to map to 2q [62]. While the discovery that Sp was an allele of Pax-3, and the subsequent identification of mutations in the PAX3 gene of Waardenburg syndrome patients [7,32,47,54,55] (discussed in Chapter two) obviated the need for a high resolution genetic map of 2q37, the PAX3-(CA)_n dinucleotide repeat polymorphism became the preferred marker to assess the degree of genetic heterogeneity.

B. Results

1. Linkage analysis of MSU4.

The proband of MSU4 (Figure 1) was identified by virtue of congenital deafness and the presence of heterochromia irides and facial hair hypopigmentation in the father.

Neither individual exhibits dystopia canthorum. Subsequent evaluation of the immediate family revealed several instances of pigmentation anomalies with no dystopia canthorum (Table 1). There is a history of heterochromia irides among first-degree relatives of MSU4-1. This family was diagnosed, therefore, as segregating for WS2.

Table 1. Phenotypes of Affected Members of Family MSU4

ID#	SN	HetI	Hyps	WF/EG	Syn	Other
1	+?				_	•
3				+		
5		+	+			**
7						***
9	I	+	+			
16	+					
18			+		+	

• = Deafness late onset; mother had white forelock; sibs have
HetT

** = Possible right sided ptosis.

••• = Unilateral pelvic kidney; other kidney rotated; undescended testes.

SN = Sensorineural deafness.
HetI = Heterochromia irides.

Hyps = Hypopigmentation of the skin.

WF/EG = White forelock and/or early greying.

syn = Synophrys.

Two caveats need mentioning before a discussion of the linkage analysis can be made. First, these phenotype

designations are tentative. No audiometric analyses has been made of any individuals in MSU4. The diagnosis of heterochromia irides in individual MSU4-9 is by hearsay. During interview, MSU4-9 reported that an ophthalmologist had told her she had

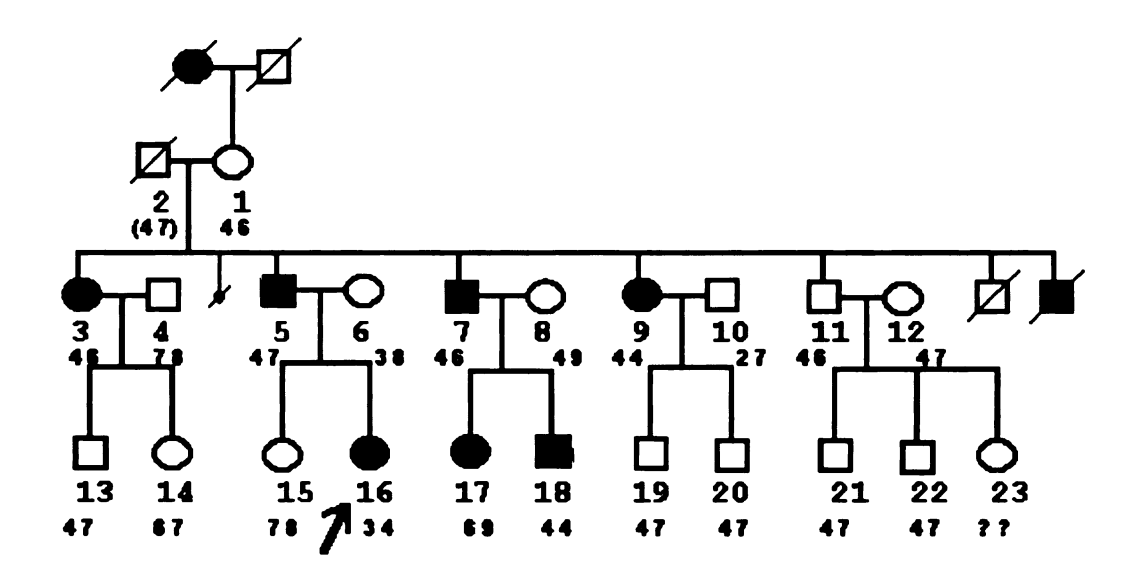


Figure 1. MSU4 pedigree. Affected individuals are indicated by darkened symbols. A grey shaded symbol indicates uncertain phenotype. The proband is indicated by arrow. Beneath each symbol is the number corresponding to the Linkage data file. Genotypes for the PAX3 dinucleotide repeat are given in small bold numbers.

heterochromia irides some years before. Dr. David Kaufman, Dept. of Ophthalmology, School of Medicine, MSU, could not confirm this diagnosis after inspection of a color slide of this individual taken recently. Dr. Kaufman did confirm the heterochromia irides of individual MSU4-5 from a color slide. The condition in MSU4-5 is reported to have been more

pronounced at an earlier age. It is plausible, then, that the diagnosis of heterochromia in individual MSU4-9 was accurate some years ago, but the appearance has diminished to the point where it is not recognizable in a photograph. In the absence of ophthalmological and audiometric exams, the two most penetrant signs in WS2 (deafness and heterochromia irides) have not been reliably diagnosed in this family [29]. The second caveat is that individual MSU4-5 has the appearance of right-sided ptosis in a still photograph. A diagnosis of "pseudo-Waardenburg syndrome"[1] cannot be ruled out.

Having stated these reservations, the results of the linkage analyses are given below (Table 2). The WS2 gene was assigned a penetrance of 57%, based on the estimate of penetrance of deafness for WS2 given by Hageman and Delleman [29]. If one assumes that the diagnosis of WS2 could be made by the presence of characters other than deafness, this figure is an underestimate. If one allows that there is a bias of ascertainment in the literature in favor of identification of individuals that may have WS2 mutations and exhibit deafness, then this figure is an overestimate.

It is quite possible, then, that the failure to reliably estimate the probability of non-penetrance in individuals whose genotypes represent obligate recombinations with PAX3 disallows interpretation of the data in this family. However, an obligate recombination occurs between PAX3 and WS2 when one considers only those

individuals with a <u>positive</u> diagnosis of WS2. An inspection of the genotypes of all offspring of MSU4-1 and MSU4-2 reveals that MSU4-2 had an obligatory genotype of {4 7} (Fig. 1). Of all of these offspring, the most reliably diagnosed are MSU4-5 (for reasons cited above) and MSU4-3 (because of the presence of a prominent white forelock). If both individuals are heterozygous for the WS2 gene, then an obligate recombination occurred between WS2 and PAX3. MSU4-3 must have inherited the 6 allele from the "affected" parent, while MSU4-5 must have inherited the 4 allele.

IOD score at Percephination Praction

Table 2. MSU4 Linkage Results

		LOD score at	t Recombinati	lon Fraction	
Marker	0.00	0.05	0.10	0.20	0.40
PAX3 *	-2.30	-1.20	-0.68	-0.20	0.05
PAX3 **	-6.78	-1.41	-0.87	-0.36	-0.02
PAX3 #	-7.50	-3.11	-2.08	-1.02	-0.15
CD3D *	-2.74	-2.39	-1.72	-0.88	-0.15
CD3D #	-8.48	-2.90	-1.80	-0.80	-0.08
D11S35 *	-2.21	-2.01	-1.60	-0.98	-0.24
D11S35 #	-4.92	-3.65	-2.60	-1.44	-0.31

Linkage of WS2 to PAX3 is excluded even if the penetrance for the +/+ genotype (i.e. the probability of a phenocopy) is given as 1/1000, the penetrance for WS2/+ is given as 57%, and the gene frequency is assumed to be 1/2100 [1]. These relaxed parameters have the effect of allowing

^{** =} Individuals 7, 17 and 18 "unknown" phenotype, and WS1 parameters.

^{# =} Individuals 7, 17 and 18 phenotypes as Table 1; WS2 parameters.

more latitude in accounting for apparent recombinations, while necessarily sacrificing power to detect linkage. For comparison, a LOD score estimate is also given for the PAX3 to WS1 evaluation, where the penetrance for WS1/+ genotype is set to 95%, the penetrance for +/+ is set to 0, and the gene frequency is assumed to be 1/42,000 [58].

This family was subsequently assayed for two chromosome 11 markers, CD3D and D11s35, both of which map near to the N-CAM (Neural - Cell Adhesion Molecule) locus [39,60]. The reasons for this are two-fold. First, control of N-CAM expression is a prominent event in the differentiation and migration of neural crest cells, and thus is a likely downstream target of the PAX3 gene product. This hypothesis is supported by the observation that N-CAM expression is altered in the neural crest cells of Sp/Sp mice [46]. Second, Tom Strachan and co-workers reported a LOD score of 2.0 for linkage between WS2 and markers near N-CAM in a British family at the Genetics of Hearing Impairment Meeting in San Diego, CA in May, 1992. Linkage analysis with both markers, CD3D and D11S35, yield negative LOD scores in MSU4 (Table 2). Further linkage analysis of this family was suspended due to the lack of reliable diagnoses .

2. Linkage analysis of MSU5.

A summary of the phenotypes of MSU5 individuals is given in Table 3, and the pedigree structure is illustrated in Figure 2. A more thorough discussion of the clinical

characteristics of affected individuals in MSU5 is given in Asher et al.[3]. The WS1 locus was previously mapped to 2q37 in this family prior to the identification of PAX3 as a candidate locus. A multi-point analysis with several RFLP markers, including one for the Alkaline Phosphatase - Placental locus (ALPP), was used to increase the informativeness. ALPP showed the greatest evidence for linkage with a LOD(Z) = 2.09 at θ = 0.0.

Table 3. Phenotypes of Affected Members of Family MSU5

ID#	DysC	SN	HetI	HypS	WF/EG	Syn
2	+	•	-	-	+	•
3	+	•	-	-	+	
4	+	•	-	-	+	-
6	+	•	-	-	+	•
7	+	•	•	-	+	+
11	+	+	+	-	+	-
14	+	+	+	+	+	+
23	+	•		-	•	+
24	+	+	-	-	-	-
29	+	•	+	-	-	-
30	+	•	+	-	-	-
37*	+	•	-	-	•	-
39*	+	•	-	•	-	-

DysC = Dystopia canthorum (defined as a/b > 0.600).

SN = Sensorineural deafness.

HetI = Heterochromia irides.

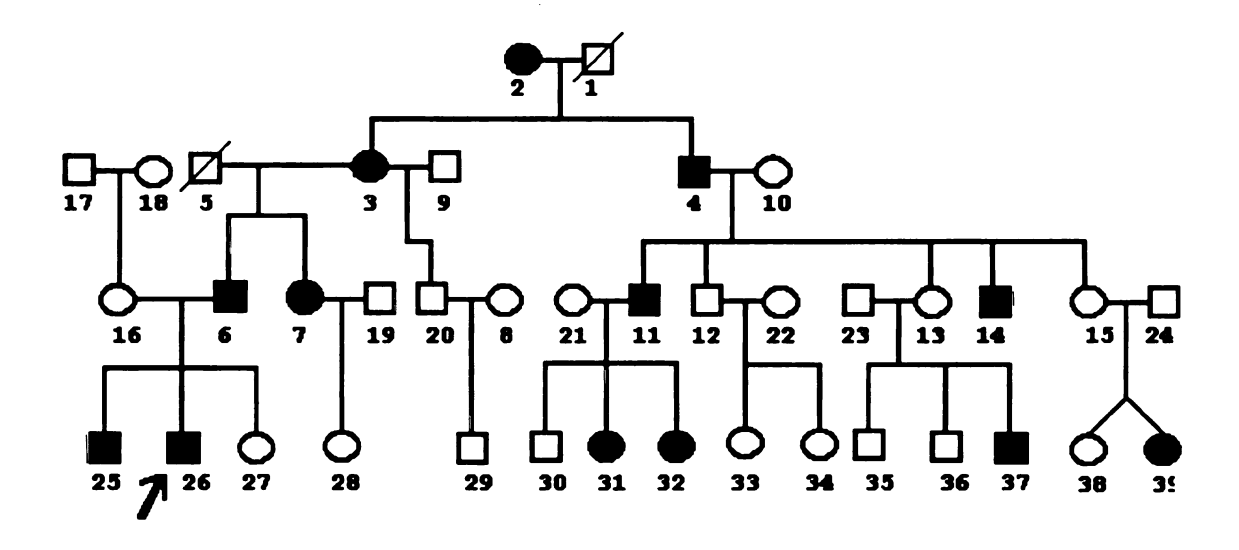
HypS = Hypopigmentation of the skin.

WF/EG = White forelock and/or early greying.

Syn = Synophrys.

* = Individuals have a/b measurements that lie in the region of overlap between the normal and affected population distributions. If affected, both would be the offspring of non-penetrant carriers.

PAX3 and ALPP show linkage in MSU5, with a LOD(Z) = 1.226 at θ = 0.11 (Table 4). A LOD(Z) = 1.32 or 1.97 at θ = 0.0 is generated for comparisons between WS1 and ALPP, depending on whether the phenotype is assigned or a quantitative measurement is used for the disease locus; in this case the a/b measurement. This ratio of the interinner-canthal distance (a) over the inter-pupillary distance (b) has a mean of ~ 0.535 in normal Caucasians, and ~ 0.695 in those affected with WS1 [3,16]. The convention suggested by Cotterman [16] has been to consider a/b measurements greater than 0.600 to be evidence of dystopia canthorum.



Pigure 2. MSU5 pedigree. Conventions are as for Figure 1.

Phenotypes are assigned by Waardenburg consortium criteria (see Appendix A). The a/b measurements are given in Table B2.

The enhanced ability to detect linkage using a quantitative measure has been demonstrated before by Lange et al.[37], who used measures of creatine kinase levels to more accurately map the Cystic Fibrosis locus. Part of the power of this method is in situations where individuals have measurements that lie at the extreme end of a normal distribution, such as individuals MSU5-37 and MSU5-39. Both individuals have a/b measurements that would classify them as dystopic according to Cotterman's criterion [16]. However, both are also the offspring of normal parents, necessitating two non-penetrant obligate carriers in the pedigree (MSU5-13 and MSU5-15). Assignment of MSU5-37 and MSU5-39 as affected forces MSU5-13 and MSU5-15 to be classified as an obligate carrier, and MSU5-15 (but not necessarily MSU5-13) thus represents an obligate recombination of WS1 with respect to ALPP. The overall result is a LOD(Z) = 1.03 at θ = 0.08. An analysis using the a/b measurement as the marker for the disease locus yields a higher LOD score partly because the Linkage program is able to include in the calculation the probability that MSU5-37 and MSU5-39 are actually normal with a/b measurements at the extreme end of the normal range. The only obligate recombination between WS1 and ALPP in the pedigree is then mitigated.

The added robustness of a quantitative measure due to the ability to resolve possible mistypings is illustrated again in the WS1 to PAX3 comparisons. The LOD(Z) score with regard to PAX3 also is substantially higher (3.6 at θ = 0.0

vs. 1.58 at θ = 0.013) if the WS1 phenotype is measured as a function of a/b rather than assigned. In this case, both MSU5-13 and MSU5-15 would have been designated as obligate recombinants with respect to PAX3, due to the greater informativeness of the PAX3 marker, if MSU5-37 and MSU5-39 were assigned as affected.

LOD Score at Recombination Fraction Comparison 0.05 0.10 0.20 0.40 0.0 PAX3 - Aff. -2.88 0.18 0.65 0.91 0.00 PAX3 - a/b 3.60 3.33 3.05 2.76 0.95 PAX3 - ALPP 1.00 1.22 1.05 0.26 -00 ALPP - Aff. -0.92 0.87 0.90 0.66 0.08 ALPP - a/b 1.97 1.75 1.52 1.04 0.15

Table 4. MSU5 Linkage Results

3. Linkage analysis of MSU6.

The assignment of phenotypes in MSU6 is particularly difficult. This is reflected in the three different versions of the pedigree displayed in Figure 3. As is reported in Table 5, two individuals have a/b ratios over 0.600 indicating dystopia canthorum. By virtue of these two (MSU6-2 and MSU6-20) this would be classified as a WS1 pedigree. Applying the Waardenburg consortium rules regarding classification (see Appendix A, Table A1) [20], would result in a pattern of inheritance represented in Fig. 3A. Individual MSU6-9 was not directly inspected, and thus his phenotype is classified as "unknown".

Table 5. Phenotypes of Members of MSU6

ID#	a/b	W	SN	WF/EG	Skin	Other
1	.538	1.75		•	•	a
2	.646	2.30	+	-	-	b
3	.500	1.63	+	-	-	-
4	.500	1.63	-	-	-	•
5	.564	1.95		•	-	-
6	.491	1.56	-	•	-	-
7	.561	1.87	+	+	-	С
8	.484	1.59	+	-	+?(d)	-
9	?	?	-	-	-	-
10	.583	2.05		-	-	-
11	.459	1.46	-	-	•	е
12	.518	1.69	-		-	-
13	.508	1.66	-	-	•	-
14	.518	1.69	-	-	+	f
15	.500	1.58	-	•	•	g
16	.545	1.80	-	•	-	h
17	.509	1.66	+	-	-	i
18	.509	1.67	+	-	+	-
19	.521	1.66	+	-	+	j
20	.653	2.22	-	+	+	k
21	.583	1.97	-	-	•	1

a/b = a/b ratio with measures that qualify for dystopia canthorum in bold.

W = Measures in dystopic and non-apparent dystopic range in bold.

SN = Sensorineural deafness.

WF/EG = White forelock and/or early greying.

Skin = Skin hypo- or hyper- pigmentation.

Other:

- a = 2 sibs with poliosis; mother had 3 miscarriages.
- b = Dizziness; 3 sibs died in infancy.
- c = Hearing loss progressive; frequent constipation.
- d = Hypopigmentation on right leg possibly due to trauma.
- e = Multiple sclerosis.
- f = Distinctly pale eyes, not seen by ophthalmologist.
- g = Severe constipation in infancy.
- h = Curved spine.
- i = Double hernia at birth.
- j = Hearing loss progressive; frequent constipation.
- k = Frequent constipation; Treacher-Collins like facies.
- l = Ears rotated.

However, the assignment of phenotype using this method is problematic in this family due to the ambiguities

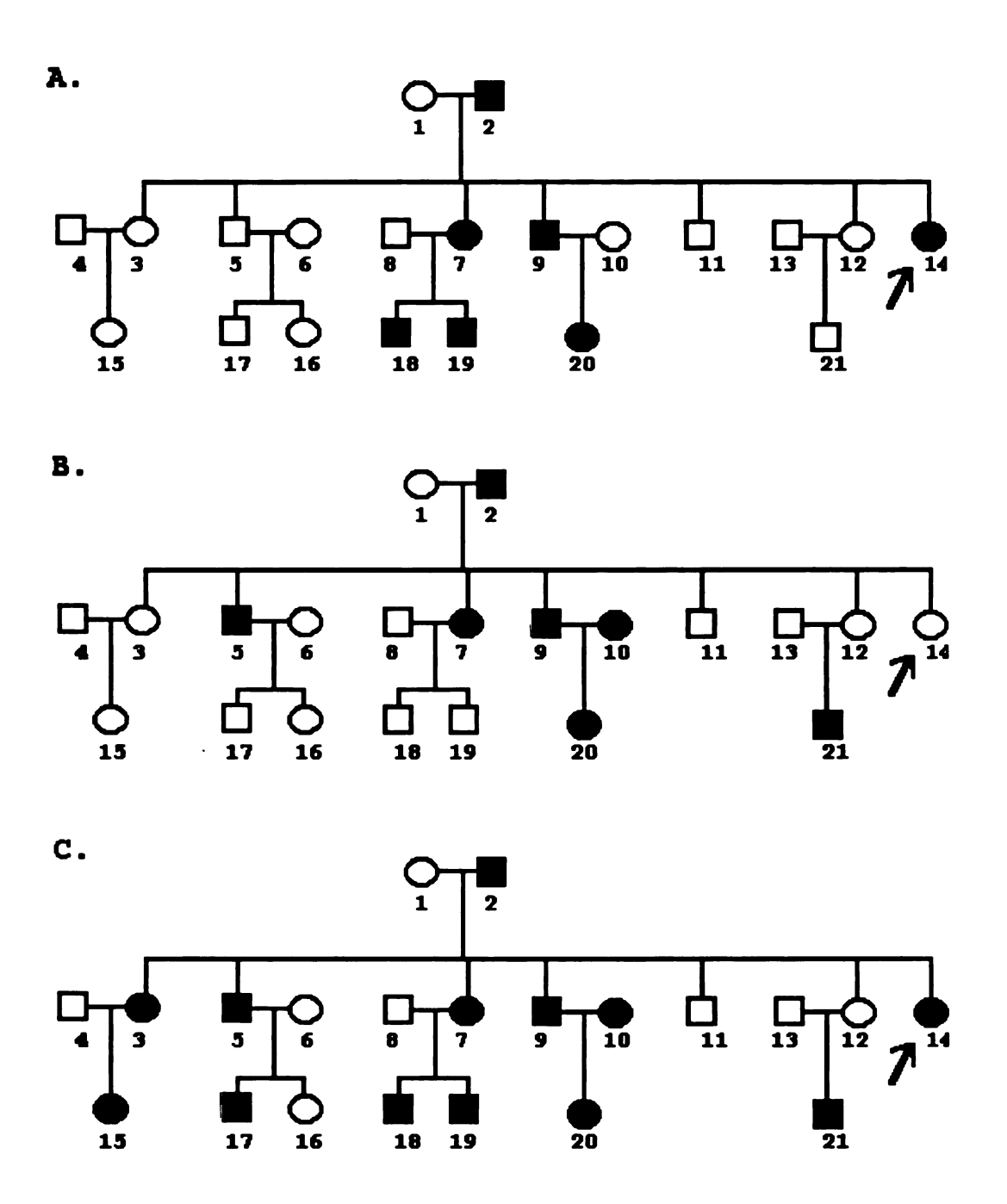


Figure 3. MSU6 pedigree structures. A. Phenotype assignment according to rules established by Waardenburg consortium (see Appendix A, Table A1). MSU6-9 is classified as "unknown", but reportedly has dystopia canthorum. B. Phenotypes assigned according to W-statistic and including the NAD category as proscribed by Arias [2]. C. Phenotypes are assigned by combination of A and B. MSU6-10 is "unknown" because she meets the W-statistic criterion only. MSU6-15 is "unknown" because of some indication of mild aganglionic megacolon but otherwise normal phenotype.

regarding the inheritance of certain of the characteristics. In particular, individuals MSU6-18 and MSU6-19 could be classified as affected because each exhibits congenital deafness and has a first-degree relative who is otherwise diagnosed as WS1 (MSU6-7, who has a white forelock and reports progressive hearing loss). However, the father, MSU6-8, has hearing impairment and reports a family history of deafness that may be genetic. Thus, the source of the deafness in MSU6-18 and MSU6-19 is questionable, and so then is the assignment of genotype, since that assignment relies upon the presence of hearing impairment.

Similarly, the presence of a white forelock in MSU6-7 and a first degree relative otherwise diagnosable as having WS1 (MSU6-2) would indicate that MSU6-7 is affected.

However, several sibs of MSU6-1 also have a white forelock, thus this trait may be segregating in the family independently of a WS1 gene. Alternatively, this suggests the possibility that MSU6-1 is a non-penetrant carrier for WS1, and that MSU6-2 is a phenocopy. There is some merit to this hypothesis, since MSU6-2 also has hypertelorism (c measurement = 90mm), which Waardenburg [58] suggested was an entity distinct from dystopia canthorum.

A resolution to these complications would be to rely on a quantitative characteristic as the measurement of phenotype. As was the case in the analysis of MSU5, this creates the opportunity for a computer program to weigh the relative probabilities that an individual is affected versus assigning an all-or-none genotype for the disease locus. However, as noted above, there are only two individuals who exhibit a/b ratios in the affected range. A linkage analysis using the a/b measurement would not be robust enough.

Arias and Mota [2] described a tri-modal population distribution of the W-statistic, and were able to use the W-statistic to reliably differentiate between affected (W > 2.07) and non-affected (W < 1.89) individuals in previously diagnosed families. Furthermore, the non-penetrant obligate carriers in these families invariably had W-values between 2.07 and 1.89, constituting the third modality of the distribution. This population was designated as Non-Apparent Dystopic (NAD). When W-values are calculated as suggested by Arias and Mota, and phenotypes are assigned according to their criteria, the result is a pattern of inheritance represented by Fig. 3B. This raises the possibility of a more robust analysis, with more "affected" individuals, but creates the additional problem of a second source for the mutation in individual MSU6-10.

A third method to more reliably assign phenotypes is to combine the consortium criteria with the W-statistic evaluation. The pattern of inheritance that results, with two modifications, is represented in Fig. 3C. Under this scheme, MSU6-10 is assigned an "unknown" phenotype since she meets the criteria for WS1 by the W-statistic evaluation but not by any other criteria. MSU6-15 is assigned an "unknown" phenotype since she reportedly has had severe episodes of

constipation, which may be indicative of some degree of aganglionic megacolon, but no other indications of WS. Three other members of the family also report repeated episodes of constipation as a clinical feature (MSU6-7, MSU6-19, MSU6-20), although this is a common complaint and need not have any relation to aganglionic megacolon. These individuals were not diagnosed using this as a criterion.

Table 6. MSU6 Linkage Results

		LOD Score at Recombination Fraction				
Comparison	0.0	0.05	0.10	0.20	0.40	
PAX3 - Aff. (I)	-10.73	-3.21	-1.92	-0.76	-0.01	
PAX3 - Aff. (II)	-4.94	-2.37	-1.57	-0.69	0.00	
PAX3 - Aff. (III)	-1.72	-1.66	-1.54	-0.98	-0.10	
PAX3 - Aff (IV)	-1.73	-1.53	-1.13	-0.53	0.00	
PAX3 - W (V)	-6.06	-2.59	-1.55	-0.60	0.00	

- I = Phenotype assigned according to consortium std.; WS1 parameters.
- II = Phenotype assigned according to consortium std.; WS2 parameters.
- III = Expanded phenotype with Father as source of mutation; WS2 parameters.
- IV = Expanded phenotype with Mother as source of mutation; WS2 parameters.
- V = Phenotype assigned according to W-statistic; WS1 parameters.

Linkage analyses of the disease locus to PAX3 were performed under the three models discussed above. In addition, the analysis was conducted using the more relaxed WS2 parameters; allowing more latitude for non-penetrant genotypes and phenocopies. Further linkage analyses were also conducted assuming that MSU6-1, and not MSU6-2, was the source of the mutation. Under all hypotheses and conditions, obligate recombinations between WS1 (WS2?) and PAX3 occur (Table 6).

4. Linkage analysis of UGM1.

Asher, Jr. during a survey of schools for the deaf on the island of Java (Figure 4). The designation "UGM" reflects the collaborative efforts of individuals from the University of Gadjah Madah, Indonesia in identifying and diagnosing individuals with Waardenburg syndrome, and in obtaining DNA samples for linkage analysis. UGM1 is an extensive pedigree, comprising 101 individuals. Only a portion of the pedigree is represented in Figure 4. This "clan" of 25 individuals is the only subgroup of UGM1 that segregates for dystopia canthorum (Table 7), and was thus chosen to be the experimental group for all linkage analyses.

Table 7. Phenotypes of Affected Members of Family UGM1

ID#	DysC	HetI	Skin	SN
6	+	+	•	•
28 *	+	•	-	•
29	+	+	+	•
30	+	•	+	+
64	+	•	-	•
65	+	+	+	-
66	+	+	+	+
67	+	+	+	+
68	+	+	+	+

DysC = Dystopia canthorum, a/b > 0.600.

HetI = Heterochromia irides.

Skin = Skin hyper- or hypo- pigmentation.

SN = Sensorineural deafness.

• _ Married into family. Classified unaffected by consortium standards.

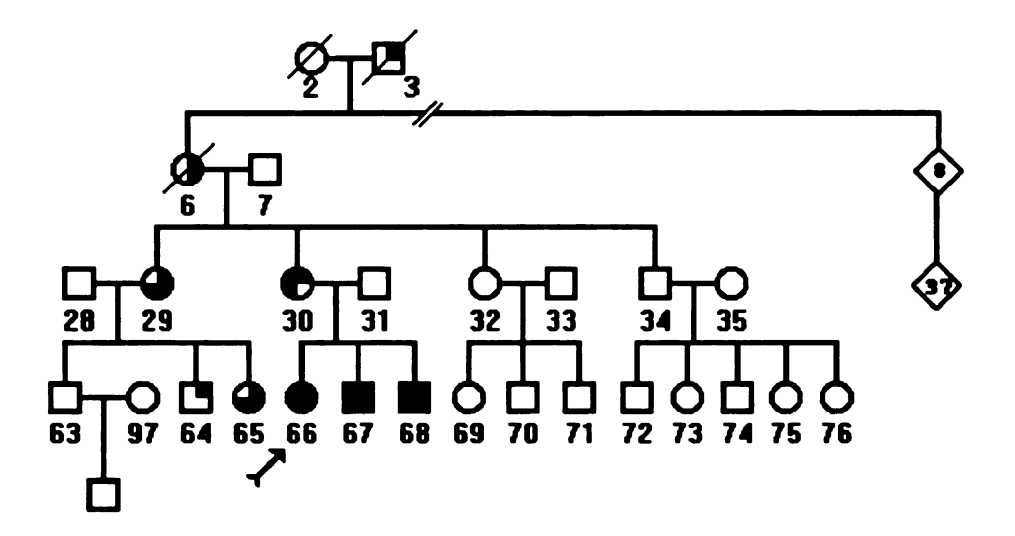


Figure 4. UGM1 pedigree. Phenotype is indicated by shaded quadrants: upper right = dystopia canthorum; lower right = heterochromia irides; lower left = hypo- or hyperpigmentation; upper left = sensorineural deafness.

Given that this is a family with mongoloid ancestry, the question immediately raised is whether the shortening of the palpebreal fissures observed is within the normal range in a population that would tend to exhibit pronounced epicanthal folds, or is a manifestation of dystopia canthorum. To address this question, the a/b measurements of 69 normal Indonesians who married into family UGM1 and another Indonesian family, UGM2 (discussed in Chapter 2), were compared to those of 516 normal Caucasoid [3]. The results of two-tailed, unpaired T-tests reveals that there is a significant difference between the a/b measurements of normal Indonesians and normal Caucasians (Table 8). There is still a significant difference, however, between Indonesians otherwise classified as affected for WS1 and normal Indonesians. Linkage analyses were performed, therefore, using a quantitative measurement for dystopia canthorum

with means and standard deviations for the a/b measurement calculated for the Indonesian population.

Table 8. Comparisons of a/b Ratios Between Indonesians and Caucasians

Affected Indonesian (n = 15) mean (std.dev.)	Indonesian (n = 15) Indonesian (n = 69)		p - value
	0.553 (0.037)	0.532 (0.034)	< 0.0001
0.684 (0.037)	0.553 (0.037)		< 0.0001

Estimates of linkage between WS1 and ALPP were largely uninformative, but yielded negative LOD scores for absolute linkage whether the disease state was assigned or calculated from the a/b measurement (Table 9). The smaller LOD score of -1.53 obtained from the a/b measurement analysis versus -0.8 obtained from the assigned phenotype analysis is presumably attributable to individual UGM1-28, who has an a/b measurement of 0.677, but is assigned an unaffected status due to the lack of any other of the criteria, including first degree relative diagnosed with WS1. But a closer inspection of the genotype data suggests that the results are actually counterintuitive. UGM1-28 has the B1B1 genotype for the ALPP RFLP marker, and thus does not contribute information to the linkage analysis, yet the magnitude of the LOD score nearly doubles with the change of affection status. The most likely explanation for this phenomenon is that the probability of detecting an obligate recombination with regard to individual UGM1-63 actually increases using

the a/b measurement, while the status of UGM1-28 is not important. This is confirmed by repeating the WS1(Affection) - ALPP linkage analysis assigning UGM1-28 the status of affected, and by repeating the WS1 (a/b) - ALPP analysis with UGM1-63 assigned the measure of 0.00 (unknown). In the former case, the LOD score at θ = 0.0 is -0.86, exactly the same as if the affection status were not changed. In the latter case, however, the LOD score at θ = 0.0 is +0.90. This suggests that the critical feature in the data set is the a/b measurement of UGM1-63, and that the reliance on a quantitative measure for the disease state increases the power to detect an obligate recombination resulting in the genotype for UGM1-63.

Table 9. UGM1 Linkage Results

Comparison	LOD Score at Recombination Fraction				
	0.00	0.05	0.10	0.20	0.40
Aff ALPP	-0.80	-0.14	0.01	0.07	0.00
a/b - ALPP	-1.53	-0.19	-0.01	0.06	0.01
Aff PAX3	2.70	2.48	2.25	1.74	0.57
a/b - PAX3	2.68	2.46	2.22	1.72	0.56

Based on this analysis, UGM1 would have been classified as one of the 55% of WS1 families that do not show tight linkage between the disease locus and ALPP [20]. However, the results of the analysis using the PAX3 marker indicate strong evidence for linkage between WS1 and PAX3 (Table 9). The LOD(Z) at θ = 0.0 is hardly affected whether the disease state is assigned (LOD(Z) = 2.7) or calculated from the a/b

measurement (LOD(Z) = 2.68). This result emphasizes the importance of not relying too heavily on the estimates for genetic heterogeneity made by Farrer et al.[20] since the marker locus used for those analyses is clearly inadequate.

C. Discussion

As Asher and Friedman [4] stated in consideration of mouse models for Waardenburg syndrome(s), there are two possible hypotheses for the observed clinical heterogeneity and variable expressivity in WS: 1) there are multiple loci for WS, each of which when mutated can give rise to the phenotype; 2) there is a single WS locus, and the phenotype is modified by multiple loci. Separate linkage analyses in single families would at once avoid the pitfall, suggested in the first hypothesis, of pooling heterogeneous data, resulting in false exclusion of chromosomal regions, while simultaneously testing the validity of both hypotheses.

The evidence of the several mouse models mentioned in the Introduction best supports the first hypothesis. Each mouse mutation segregates independently and causes some aspect of the clinical constellation defining the syndrome, but does not in itself account for the full range of the phenotype (to the extent that any have been assayed for the full range of clinical features). However, it must be remembered that laboratory mouse strains are highly inbred, and it is likely that the alleles at putative modifying loci would be fixed in the population. The fact that only a subset of the possible traits segregates in a strain may be due more to a fixed set of modifying loci in each strain than it is to the presence of multiple "WS" genes.

Support for the second hypothesis comes from the observation by Dr. James Asher (unpublished data) that when

the Sp^d allele (which originated in a Mus musculus background) is crossed into a Mus spretus background, the resulting hybrids exhibit dystopia canthorum, a trait not previously observed. Thus, the penetrance of the gene for one of the traits depends on the genetic background in a strain. Since the various WS clinical types are defined by the inclusion or exclusion of certain traits comprising a rather broad set, the particular subset of clinical features exhibited by a given family may be largely dependent on allelic states at other loci.

The identification of Pax-3 as the Sp locus did not resolve this issue [18,19]. As a probable transcription factor acting on numerous downstream genes expressed in neural crest cells [27], mutations in PAX3 might be responsible for the full spectrum of WS clinical features. In addition to the several mutations in PAX3 that are purported to give rise to WS1, there are now PAX3 mutations that presumably give rise to WS2 [55] and WS3 [32]. The reported WS2 case is arguably WS1, since one of the family members has a W-index value > 2.07. The WS3 diagnosis, however, is clearly accurate, since several individuals in the family have upper-limb deformities.

With regard to the relationship between PAX3 and the various WS subtypes, there are three possibilities: 1) It is possible that the variance and clinical heterogeneity of WS are due purely to the normal chance events of a mutant gene exerting its effects on a large population of cells that

must traverse through, and interact with, a complex environment. 2) It is also possible that mutations of PAX3 are the primary causes of all WS, and the variance and clinical heterogeneity is due to the allelic states at various downstream target genes. The former and latter possibilities are, of course, not mutually exclusive. But it also remains a possibility that 3) a mutation at one or several of the hypothesized downstream targets could be necessary and sufficient to account for some instances of WS.

Observed recombinations between a PAX3 allele and the "disease locus" when the resulting phenotype is normal cannot distinguish among these three possibilities. The recombination may not be real, but only apparent because of non-penetrance or difficulty in diagnosis. Or the phenotype may be normal due solely to chance events suggested under possibility number 1 despite the presence of a PAX3 mutation. But if a recombination occurs between a PAX3 allele and the disease locus in the case that the resulting phenotype is unambiguously classifiable as WS, then the best explanation (barring a new mutation or phenocopy) is that another WS locus exists.

The linkage analyses of MSU4 and MSU6 both provide evidence of the latter sort. The evidence in MSU4 is stronger because of the difficulties in assigning phenotypes, or even determining the number of mutant genes segregating, in MSU6. In MSU4, an obligate recombination

occurs when one considers the PAX3 genotypes among reliably diagnosed affected individuals. When a more complete clinical examination is made of the individuals in MSU4 additional recombination events may be detected. This pedigree might then be suitable for detecting positive evidence for linkage of genetic markers to a WS2 locus.

To date, the best evidence for genetic heterogeneity of WS is Farrer et al.[20]. This analysis of a pooled data set comprising 44 kindreds, including MSU5, found evidence for genetic heterogeneity when considering linkage of WS1 to the RFLP marker for ALPP. However, there are at least two weaknesses to the analysis that argue for withholding judgement on this issue. Both are illustrated in the linkage analyses of MSU5 and UGM1.

First, the consortium analysis relied on the recombination information provided solely by ALPP. It now appears that ALPP is ~10 cM from the WS1 locus. As can be seen from a comparison of the analyses of UGM1 and MSU5, it is quite possible to obtain a negative LOD score with respect to ALPP in one family and a positive one in another family, when both families give positive and significant LOD scores with respect to PAX3. Also, the RFLP marker for ALPP is often uninformative. Moreover, there is a pseudogene of ALPP whose location is unknown [42], and an ALPI locus on 2q35 that presents a similar restriction pattern on Southern blots to ALPP. There exists, then, considerable opportunity for mistyping of the ALPP locus. The consortium is currently

collecting PAX3 genotyping data for the entire data set, as well as data for other highly informative markers thought to be near PAX3.

The second weakness of the consortium analysis is that the criteria for assignment of phenotype may not have been consistently applied. This is unavoidable in any collaborative effort, but the diagnoses for WS are particularly difficult since few of the characteristics can be quantified. Ideally, the phenotypes would have been quantified, both as a means of ensuring uniformity in clinical classification, and as a means of adding robustness to the linkage analysis. As demonstrated in the linkage analysis of MSU5, the ability to assign probabilities for individuals to be either affected or at the extreme end of a normal distribution can have a significant impact on the analysis. Two obligate recombinations with respect to PAX3 in MSU5 were mitigated by consideration of the amount of overlap between the a/b measurement distributions of the normal and affected populations.

The best assessment, then, of the degree of genetic heterogeneity in WS will be the consortium analysis currently being done. Ideally, this analysis will include a quantitative measure as a marker for the disease locus whenever possible. Most important will be the identification of obligate recombinations involving individuals who clearly have the WS phenotype.

II. CHAPTER TWO: Mutations in PAX3 associated with Waardenburg syndrome.

A. Introduction

The mapping of WS1 mutations to 2g37 [3,22] gave greater weight to the proposition that the mutation Sp was the murine equivalent of WS1.[4] When Epstein et al.[18] subsequently demonstrated that the allele Sp^{2H} was a mutation of the Pax-3 gene, the problem of identifying the WS1 gene was transformed from one of positional cloning to that of testing a candidate locus. Tassabehji et al.[54] and Baldwin et al.[7] demonstrated sequence changes in human PAX3 in individuals with classical WS1 soon after. Both mutations created missense messages: an 18 bp deletion retaining the reading frame and a proline to leucine replacement. Both mutations occur in the highly conserved paired box, which encodes a DNA binding domain [57], while presumably leaving intact the rest of the protein, including the two other motifs common in DNA-binding proteins (an octapeptide sequence and a homeo box) [27]. The effects that these mutations would have on normal PAX3 protein function are necessarily speculative, since the target genes of this transcription factor have not been identified. The question remains open, then, as to whether the mutations exerted their dominant effects by: 1) producing DNA-binding proteins with altered specificity; 2) producing mutant proteins that interact with normal proteins to produce a negative-dominant

effect; or 3) producing functionally negligible proteins resulting in haploinsufficiency in a concentration sensitive milieu. The most direct method for addressing this question is to characterize additional mutations that may suggest the mode of molecular pathology.

One strategy for detecting mutations is to sequence the PAX3 gene in affected individuals. The effort involved would be considerable given that the PAX3 cDNA is expected to be approximately 1,437 nucleotides long based on the murine cDNA [27]. However, the only human sequences available at the time of this study were represented by HuP2, a genomic clone containing three of the predicted five exons, or 134 of the predicted 479 codons [14]. Given the fact that an assay for possible mutations in all of the coding and non-coding sequences of PAX3 was not possible, and given the estimate that mutations in 55% of families are not linked to 2q37 markers [20], a more efficient method for detecting possible mutations in the three available exonic sequences of PAX3 was necessary.

Our strategy for identifying WS1 mutations in PAX3 was three-fold. DNA fragments containing exons 2, 3 and 4 of were amplified by the polymerase chain reaction (PCR) and either: 1) electrophoresed on native polyacrylamide gels to detect heteroduplex DNA, which are DNA fragments formed from the mismatched strands of wild type and mutant alleles, and exhibit different mobility from homoduplex DNA due to looping of the mismatched sequences; or 2) denatured and

then electrophoresed on native polyacrylamide gels to detect single strand conformation polymorphisms (SSCPs), which occur due to the assumption of sequence-specific secondary structures as the denaturing solution carrying the single strands becomes increasingly diluted during migration through the gel. A major pitfall of any PCR-based technique to detect mutations is the possibility that the mutant allele will not PCR amplify because of a deletion or mutation in the primer sequences. Therefore 3), 32P - dATP labeled PCR fragments amplified from wild-type exons of PAX3 were used as probes to Southern blots of endonuclease restricted genomic DNA in order to detect large rearrangements, potentially involving intronic sequences or deletions encompassing the PCR primer sites.

B. Results

Representative DNA samples from thirteen different families segregating for Waardenburg syndromes were included in the SSCP analyses (Figure 5). In each case, the proband of a family was used, with the exception of MSU6. For MSU6 both the parents were used (MSU6-54 and MSU6-55) because of uncertainty of the proband's phenotype and the uncertainty of the origin of the mutant allele. For MSU4 a distantly related individual (MSU4-25) was included in addition to the proband (MSU4-4) because of the severity of the phenotype and the possibility that more than one mutant allele was segregating in the family. Table 10 summarizes the phenotypes of individuals whose DNA was used in this analysis.

Initial results comparing heteroduplex gels with SSCP gels demonstrated the SSCP technique to be more sensitive in detecting sequence variations, and heteroduplex assays were discontinued. SSCP gels run at 8 Watts at room temperature were comparable to gels run at 12.5 Watts at 4°C, and only the former are shown in Figure 5. Single strand conformation polymorphisms for the exon 2 containing fragment (PCR primers TF30 & TF32) were observed for MSU3-9, MSU6-55, and UGM2-24. The polymorphism for MSU6-55 was shown to be due to an intronic Hae III polymorphism [7] by restriction analysis. No polymorphisms were detected for exon 3 or exon 4 PCR fragments.

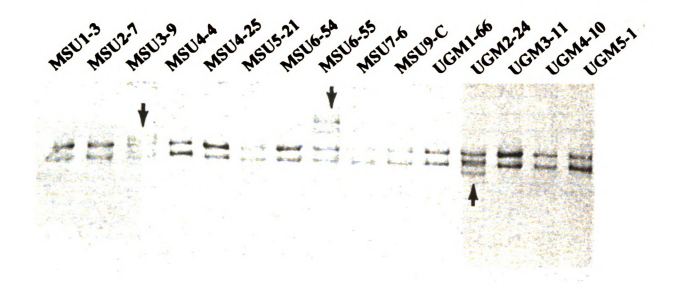


Figure 5. SSCP Analysis of PAX3 Exon 2 PCR Fragments in Affected Individuals. The 35s-dATP labelled PCR fragments were generated from genomic DNA using primers TF30 and TF32 (see Table A2). Individual IDs are indicated above lanes. All individuals are the probands for the given WS family, with the exceptions of: MSU4-25, which is a severely affected third cousin of MSU4-4; and MSU6-54 and MSU6-55, which are the parents of the proband MSU6-70, and are substituted because of uncertainties regarding phenotype for MSU6-70 and uncertainty of the origin of the mutation. The normal 535 bp PCR fragments migrate in a simple two-band pattern when electrophoresed through 1x MDEE gels (AT Biochem). Fragments generated from other alleles create additional bands indicated by arrows. The faint additional bands from MSU3-9 are due to an allele containing a 1 bp insertion. The extra band from UGM2-24 is due to an allele containing a 14 bp deletion. The extra set of bands from MSU6-55 are due to an allele containing a nucleotide substitution in the intron sequences of the PCR fragment.

Person ID Broad Nasal a/b HetI WF/EG Synophrys Root MSU1-3 Х Х 600 Х Х Х MSU2-7 Х Х 740 MSU3-9 .700 X Х Х X Х MSU4-4 528 X X MSU4-25* NA X MSU5-21 673 MSU6-54 .538 X X MSU6-55 646 X MSU7-6 NA Х X Х X MSU9-C NA X** Х Х X Х UGM1-66 714 X** UGM2-24 .700 Х X X** Х Х Х Х UGM3-11 .700 UGM4-10# X** X X X X .618

X

Table 10. Phenotypes of WS Subjects

X**

. 586

UGM5-1

The exon 2 PCR fragments for MSU3-9 and UGM2-24, exon 3 fragments for UGM2-24, and exon 2, 3 and 4 fragments for MSU5-21 and UGM1-66 were cloned into the pCR 1000 (Invitrogen) vector and both strands of multiple clones were sequenced.

Exon 2 of the mutant allele in MSU3-9 contains a guanine insertion at the first nucleotide of the paired domain (Figure 6). This insertion would presumably cause a shift of the reading frame and the creation of a premature translation codon in exon 3, resulting in a truncated protein product lacking any functional paired domain, octapeptide sequence, or homeodomain. This insertion creates an AvaI restriction site (CTCGGG) in the mutant allele.

^{*} Other characteristics include: cleft lip and palate, microcephalus, absence of nasal bone, left hydronephrosis, small penis, mental retardation.

^{**} Indicates isochromiac hypoplastic blue eyes.

[#] Mentally retarded, abnormal facies, abnormal gait.

Figure 6. Sequence of Mutant PAX3 Allele Responsible for WS1 in Family MSU3. The left panel shows a partial sequence from the normal allele PAX3 PCR amplified from individual MSU3-9. The right panel is the sequence from the mutant allele PCR amplified from MSU3-9. The guanine insertion is indicated by an asterisk. Both strands of multiple independant clones representing the mutant allele were sequenced.

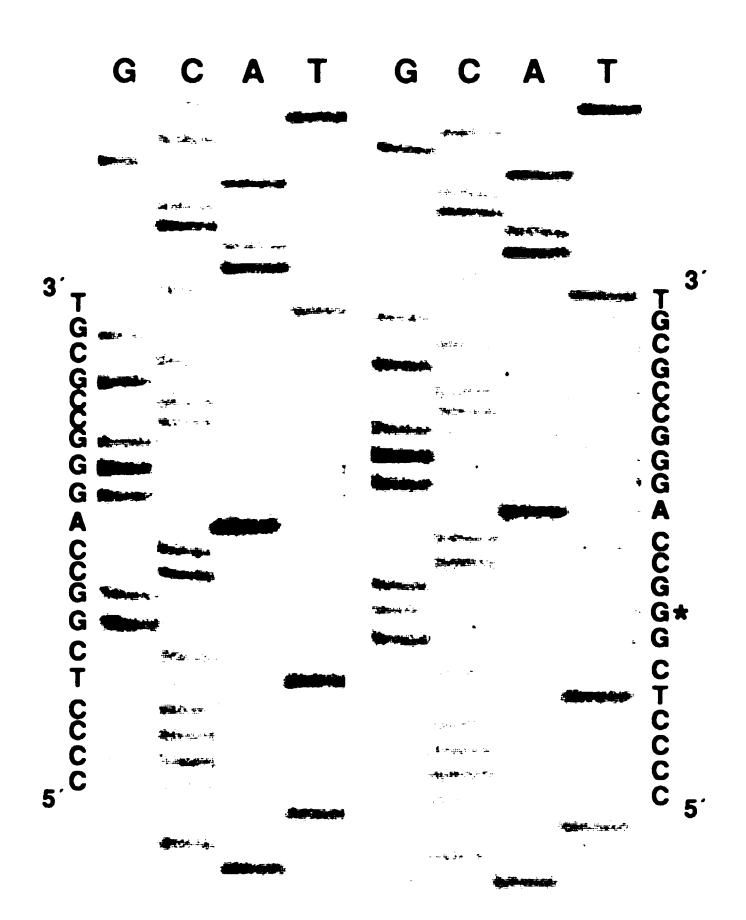
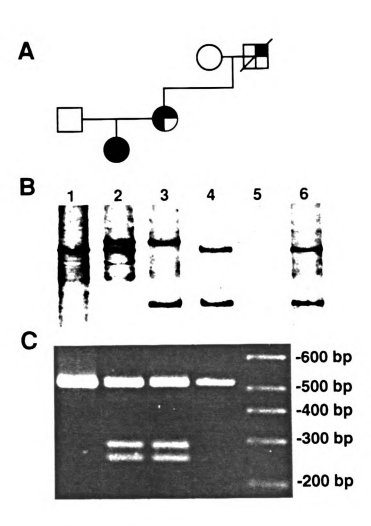


Figure 7. Confirmation of the Segregation of a Mutant Allele in Family MSU3. A. The pedigree structure of MSU3 with individual symbols overlying the corresponding lanes for B and C. Phenotypes are represented as filled quadrants in the pedigree diagram: upper right = dystopia canthorum; lower right = heterochromia iridis; lower left = hypo pigmentation; upper left = sensorineural deafness. B. Silverstained gel showing the SSCPs of the exon 2 PCR fragment amplified from: 1) MSU3-10; 2) MSU3-9; 3) MSU3-8; 4) MSU3-15; 5) MSU3-16 (blank); 6) an individual previously demonstrated to be heterozygous for a HaeIII polymorphism described by Hoth et al.[32]. Thus, MSU3-10 exhibits the normal pattern; MSU3-9 exhibits an additional band presumeably representing the fragment from the mutant allele; MSU3-8 also exhibits the additional band, and a lower band which is a result of the polymorphism at an intronic HaeIII site; MSU3-15 is heterozygous for the HaeIII polymorphism. The extra G occurs at the first nucleotide of the paired box and creates an AvaI digestion site. C. PAX3 exon 2 fragments PCR amplified from genomic DNA samples from affected and unaffected individuals in family MSU3. Fragments were digested with AvaI and electrophoresed on a 3% Nusieve 3:1 gel in TBE buffer. PCR fragments from the normal allele migrate at 535 bp. Fragments from the mutant allele migrate at 289 bp and 247 bp. Lane 5 contains a molecular weight marker with sizes indicated at right.



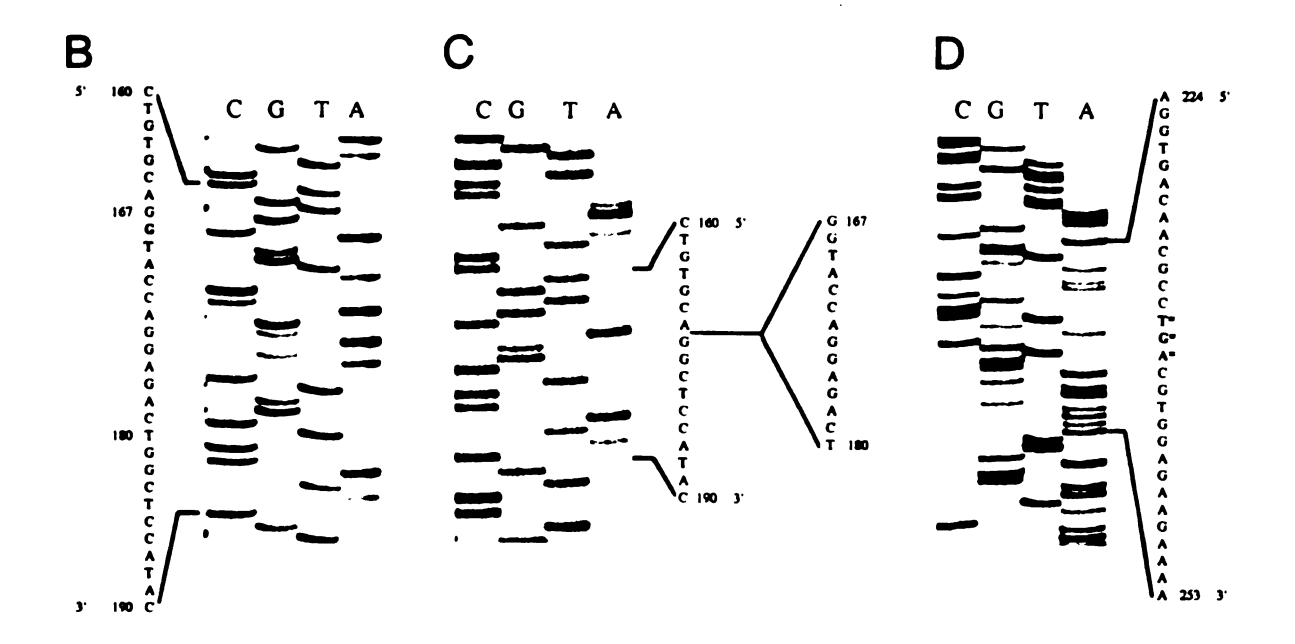
Therefore, we confirmed that this insertion is not a random PCR or a cloning artifact by AvaI digestion of total PCR amplified DNA and electrophoretic separation on an agarose gel. Genomic DNA amplified from unaffected individuals and digested with Ava I displayed only a single band of 535 bp, while that of affected individuals display a 535 bp fragment representing the normal allele, and two fragments of 289 bp and 247 bp representing the mutant allele (Figure 7).

Exon 2 of the mutant allele in UGM2-24 contains a 14 base pair deletion beginning at nucleotide 167 of the paired domain (Figure 8A & B). The deleted segment includes a RsaI restriction site beginning at nucleotide 168. All available DNA samples from the UGM2 family were subsequently assayed on a Southern blot (Figure 9) probed with ³²P-dATP labeled exon 2 PCR fragments. Perfect cosegregation of a unique 2200 bp fragment with the mutant phenotype was observed (Lod(Z) =3.82, θ = 0.0). The 2200 bp fragment was not seen in 18 normal unrelated Indonesians nor in 16 normal unrelated Americans in subsequent experiments. This deletion causes a frame shift in exon 2 which results in a UGA stop codon in exon 3 (Figure 8C). The position of the stop codon was confirmed by sequencing exon 3 from the same affected individual (Figure 8D). The deduced translated product would lack 57% of the paired domain and all of the octapeptide sequence and homeo domain.

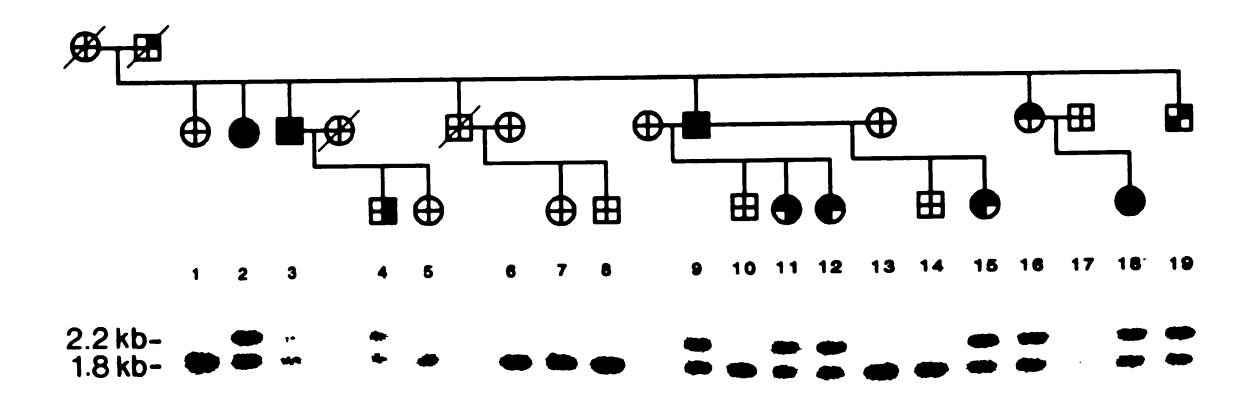
No SSCPs, heteroduplex formations, or sequence alterations were detected in any of the exons PCR amplified from individuals MSU5-21 and UGM1-66.

Figure 8. Sequence of the Mutant PAX3 Allele Segregating in UGM2.

A. A comparison of the mutant and wild type sequences of the paired box of PAX3. The nucleotide sequence begins with the first codon of the PAX3 paired box according to Burri. et al [14]. The wild type amino acid sequence is given in the top line, and the mutant amino acid sequence is given in the bottom line. Dashes indicate amino acids identical to the wild type sequence. The 14 bp deletion is indicated by arrows and intervening ellipses. The new reading frame created by the deletion is indicated by brackets beneath the nucleotide sequence. The exon 2/exon 3 border is indicated by <>. The RsaI restriction site deleted in the mutant allele is shaded. The putative first alpha helix region is underlined. B. A partial nucleotide sequence from the wild type exon 2. C. Nucleotide sequence from the mutant exon 2. D. The exon 3 sequence from an affected individual. The new termination codon in exon 3 created by the frame shift mutation is indicated by *. The sequence data represented in B, C and D were each confirmed for both strands of three independent clones.



Pigure 9. UGM2 Pedigree and Southern Blot Detection of a Mutant PAX3 Allele. A Southern blot of RsaI restricted genomic DNA from members of family UGM2, probed with \$32P-dATP\$ labelled exon 2 PCR fragments from a wild type PAX3. This PAX3 probe hybridizes to a 1.8 kb fragment from the wild type allele, and to a 2.2 kb fragment from the mutant allele. Pedigree members are illustrated above the corresponding lanes. Phenotypes are represented as filled in quadrants: upper right = dystopia canthorum; lower right = heterochromia iridis; lower left = hypo- or hyperpigmentation; upper left = sensorineural deafness.



C. Discussion

The spatial and temporal pattern of expression of the murine gene Pax-3 in developing mouse embryos is coincident with regions in which neural crest cells originate and migrate [27], which is consistent with the neural crest origin of tissues that are altered in WS1. Pax-3 contains both a paired box and a homeo box, which are highly conserved sequences that encode DNA binding domains, and is thus thought to encode a transcription factor responsible for pattern formation in the developing embryo. Thus, the discovery that Sp^{2H} is an allele of Pax-3 [18] promised a possible resolution to the problem of variable phenotype in Waardenburg syndrome. As a transcription factor, PAX3 proteins would interact with a variety of other genes, many of which would be expected to be involved in normal neural crest cell differentiation. The manner and degree in which a mutant PAX3 would interact with these downstream target genes could be heavily influenced by different alleles at the downstream loci or different alleles of PAX3. Thus, a gene affecting neural crest cell populations prior to their migration and differentiation offers an explanation for the pleiotropy of WS1, and the candidate locus' status as a transcription factor interacting with many other genes could account for the variation in expressivity. This model could possibly account for all of the clinical heterogeneity. Conversely, the identification of the downstream targets for PAX3 could provide the best candidates for other WS loci if

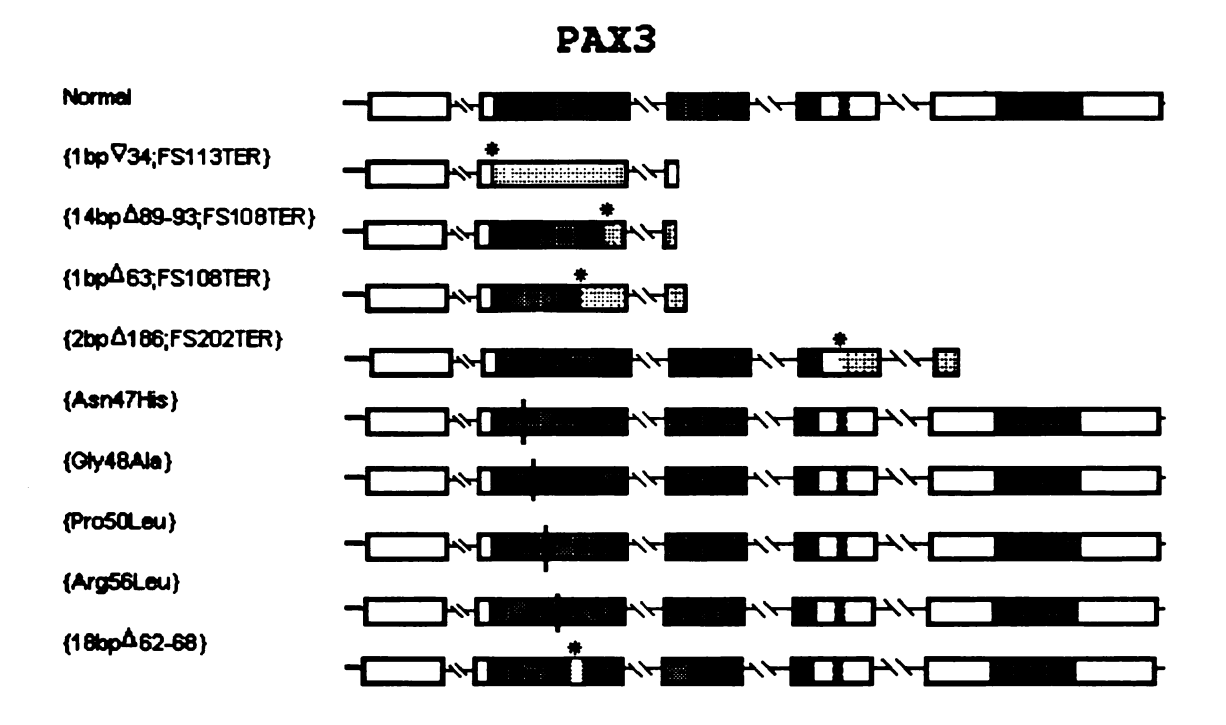
the clinical heterogeneity in fact reflects genetic heterogeneity.

A first step in dissecting the molecular pathology is to assess the functional consequences of mutations on normal protein function, and correlate mutant genotypes with phenotypes.

Exons 2, 3 and 4 of PAX3 encode a paired domain of the prd - gsb type. Exon 4 also encodes an octapeptide sequence conserved in DNA-binding proteins, and exon 5 encodes a homeodomain [27,32]. In other species, it has been demonstrated that the paired and homeo domains have DNA-binding properties, and are frequent motifs of transcription factors involved in developmental regulation [27,28,50,57]. The mechanisms by which these domains bind DNA and affect transcription control have not been completely determined.

The paired box encodes three putative alpha helices [12] of variable amino acid sequence, while the regions surrounding the helices are highly conserved. Treisman et al.[57] demonstrated in vitro that disruption of the first helix in the Drosophila prd gene abolished the DNA binding capacity of the paired domain to a specific recognition sequence, while various mutations in either the second or third helices did not impair DNA binding of the paired domain. Substitution of a glycine residue for serine at position 48 in the highly conserved region 5' to the first helix also abolished DNA binding. This is the same substitution that occurs in the mouse gene Pax-1 and causes

the *undulated* (*un*) phenotype [8,15]. Treisman et al. reasoned that amino acid variation in the highly conserved regions would result in loss of DNA binding activity due to changes in the three dimensional folding of the protein.



Pigure 10. Summary of all WS mutations in PAX3 published to date. Diagram represents the translated sequences of PAX3 according to Goulding et al.[27]. Grey shading represents paired domain. The octapeptide coding sequence in exon 4 is represented by hatched shading. Black shading in exon 5 represents the homeo domain. Asterisks above diagrams indicate points of deletions or insertions. Reading frame shifts are represented by stippled shading, ending in new translation termination codons. Vertical lines through the diagram indicate positions of missense mutations. Allele designations for each diagram are given at left. The nomenclature conventions are explained in Appendix D. References for each mutation can be found with their descriptions in the text.

In PAX3, the putative first alpha helix region of the paired box extends from position 56 to 64 (numbering from amino acid sequence determined by Hoth et al.[32]. The

deletion described by Tassabehji et al.[54] extends from codon 62 to 68 (PAX3{18bp\(Delta 62-68\)}). The missense mutation reported by Baldwin et al.[7] occurs at codon 50 (PAX3{Pro50Leu}) where, by analogy to the prd and Pax-1/un mutations, it may effectively abolish the DNA binding capacity by altering the tertiary structure surrounding the first alpha helix. Because both of these PAX3 mutations maintain the downstream amino acid sequences, the functional impairments of the PAX3 protein are not immediately apparent.

The WS1 mutation segregating in family UGM2 deletes 14 nucleotides beginning at codon 89 causing a frame shift and thus a translation termination signal 19 codons later (PAX3{14bpΔ89-93,FS108TER}). The first alpha helix is left intact in the mutant protein, while the remainder of the paired domain, including the two helices comprising amino acids 113 to 138, and the entire predicted homeo domain are removed. The deduced mutant PAX3 peptide contains only 163 amino acids of the predicted total of 479.

It is possible that the truncated PAX3 protein in WS1 individuals of UGM2 is unstable and is degraded rapidly, or lacks the nuclear targeting sequences. In either case, the result would be haploinsufficiency of the PAX3 protein. However, if the truncated protein is transported to the nucleus, it might retain its DNA binding ability by virtue of an intact first alpha helix in the paired domain, and could conceivably interfere with normal PAX3 functions. The

mutant PAX3 allele in UGM2 would then represent a trans dominant negative mutation. A series of binding assays of the normal and truncated proteins to known paired domain DNA recognition sites would be required to assess the likelihood of the latter proposition.

Since a full length cDNA for PAX3 is not currently available, electrophoretic mobility shift binding assays for normal and truncated PAX3 proteins are not yet possible. However, Goulding et al.[27] performed such assays for the Pax-3 protein and demonstrated that it binds the e5 sequence of the Drosophila even-skipped gene which contains recognition sites for both the paired domain and homeo domain. While both recognition sequences were necessary for high affinity binding by Pax-3 and Pax-1 proteins, truncated Pax-1 proteins are capable of binding DNA in vitro at low efficiency [15,27]. The various truncated proteins they assayed did not, however, include one in which only the first helix in the paired domain was left intact. Thus, it is conceivable that the truncated PAX3 protein lacking the entire homeo domain could occupy normal binding sites, but the question remains whether a single helix in the paired domain is sufficient for DNA sequence recognition and binding. It is possible that the truncated protein product may compete with normal PAX3 proteins for binding with associated factors that are necessary either for normal DNA binding or for exerting normal transcription control. The

effects of reduced PAX3 production would thus be compounded by reduced availability of associated factors.

If high affinity binding of the PAX3 protein to its DNA target sequences requires the interaction with additional factors, it is most likely that the truncated (PAX3{14bp\Delta89-93,FS108TER}) protein lacks the necessary binding domains. Whether this would result simply in the loss of normal transcription control, or in the gain of novel transcription control is impossible to assess at this point.

The mutation segregating in MSU3 adds insight to this question. It also causes a shift in the reading frame (PAX3{1bp ∇ 34,FS113TER}). However, the one base-pair insertion occurs at the <u>first</u> codon of the paired box, eliminating the reading frame for the entire paired domain. The resulting peptide would lack paired domain as well as lacking an octapeptide sequence and homeo domain. It is highly improbable that this peptide retains any DNA-binding capacity, although it is still possible that it can interact with associated factors via the peptide coded for by the first exon.

It is instructive to note that the Splotch phenotype in mice can be caused by the complete deletion of a Pax-3 allele $(Sp^r/+)[10,18]$. Another allele of Pax-3 that causes the Splotch phenotype (Sp^{2H}) codes for a truncated protein [18]. In this case, a deletion causing a frame shift resulted in a premature termination codon in the homeo box downstream

from the paired box. The predicted protein product has a normal paired domain and a partial homeo domain. The phenotype of $Sp^{2H}/+$ mice appears to be the same as that of $Sp^{r}/+$.

This relation of genotype to phenotype is consistent with other known mutations in PAX genes. For example, two of the three mutations that cause the dominant small eye phenotype in mouse are nonsense mutations in Pax-6 creating truncated proteins, and the third is a deletion heterozygote [31]. Again, the phenotypes are indistinguishable. Aniridia, a condition in humans homologous to small eye in mouse, is the result of a homozygous deletion in one case, and a heterozygous nonsense mutation in another [56]. These observations suggest that the observed traits in the mutant phenotypes are caused by insufficient dosage of functional proteins.

The two mutations described in this thesis,

PAX3{1bp∇34,FS113TER} and PAX3{14bpΔ89-93,FS108TER}, produce

virtually the same phenotype as those produced by

PAX3{Pro50Leu} and by PAX3{18bpΔ62-68}, even to the extent

that both the UGM2 family and the Brazilian family

investigated by Baldwin et al. have an unusually high

penetrance for hearing impairment (75% and >78%

respectively). All of the affected individuals show

classical WS1 characteristics. The addition of the two

mutations described in this thesis, and others recently

published [19,55], argue strongly for haploinsufficiency to be

the primary cause of the WS1 and Sp phenotypes. The mutations PAX3{18bp\(Delta\)62-68} and PAX3{Pro50Leu}, therefore, probably result in functionally inactive proteins. The variable penetrance and expressivity could then be attributed to the chance events of organogenesis inherent in a system where a population of migratory cells interacts with a complex extracellular environment, which is in turn influenced by multiple genes.

The reduced dosage effect could be magnified if PAX3 normally autoregulates its own expression, as has been demonstrated for other homeo domain proteins such as Ubx in Drosophila [30]. The mutant allele might dilute the upregulation effects by failing to bind factors that promote the further PAX3 production. In addition, a threshold level of PAX3 activity may be needed before a cell can commit itself to a particular developmental pathway. Reduced dosage of PAX3, magnified by obstruction of normal up-regulation mechanisms, might delay the attainment of threshold levels beyond the boundaries of narrow developmental windows. This would result in a defect of heterochrony, or the timing of developmental events. In fact, neural crest migration from neural tube explants is delayed in Sp/Sp mice [46]. It is possible that the neural crest cells of mutant embryos retain the capacity for normal migration and differentiation, and that the surrounding tissues retain the capacity to support neural crest immigration, but that the tissues develop out of phase with each other. A similar

situation is seen in the white axolotl mutant, in which the subepidermal matrix develops out of phase with migrating melanoblasts [49].

As mentioned in Chapter 1, the clinical description in the literature of Waardenburg syndrome allows for the interpretation of a single gene defect with epistatic influences. An observation in support of this idea is the appearance of dystopia canthorum, a trait not previously known to be associated with *splotch*, in mice when Sp^d is crossed into a different genetic background than which it originated in (J. Asher, unpublished data).

Given that the differentiation of numerous tissues are affected by PAX genes, it may be that differences between organisms heterozygous for PAX point mutations and organisms heterozygous for PAX deletions would be revealed upon closer inspection of other traits in the phenotype. It is still possible that the high variation in expressivity among WS1 families is not due to complex epistatic interactions, nor stochastic events, but rather to allelic mutations at PAX3, some of which result in haploinsufficiency of PAX3 while others result in varying degrees of a trans dominant negative effect. One might expect that missense mutations at PAX3 would produce more severe phenotypes, since the mutant protein might have altered specificity thereby affecting numerous target genes. The mutation PAX3{Asn47His} described by Hoth et al.[32] lends weight to this hypothesis, since it occurs in an individual with type 3 Waardenburg phenotype.

The is contrary to expectations, since most of the previously described WS3 cases were most likely examples of a contiguous gene syndrome (see Introduction). But such speculation should be tempered by the consideration of the other four missense mutations and the classical type I phenotypes that they produce.

In summary, there does not yet appear to be a clear correlation between genotype and phenotype for the mutations so far described. This both reflects the paucity of information on normal PAX3 function and regulation, and the likelihood of epistatic effects from other, unidentified, loci.

III. Appendix A.

Materials and Methods

1. Evaluation of Subjects.

Unless otherwise specified, subjects were classified according to the criteria established by the Waardenburg consortium [20]. To be considered affected, an individual must exhibit either: a) at least two of the major criteria or b) one of the major criteria and two of the minor criteria.

Table A1. Waardenburg Consortium Criteria

Major:

- 1. Sensorineural deficit
- 2. Iris pigmentary abnormality:
 - a. heterochromia irides
 - b. segmented iris/iris bicolor
 - c. "sapphire blue" iris confirmed with slit lamp
- 3. Hair hypopigmentation
 - a. white forelock, at any age, need not be permanent
 - b. white hairs elsewhere on body
- 4. Dystopia canthorum, defined as W index > 2.07 (Note that this does not include the non apparent dystopic {NAD} class defined by Arias and Mota to be 2.07 < W > 1.89)
- 5. First degree relative otherwise classified as WS1

Minor:

- 1. Congenital skin hypopigmentation
- 2. Synophrys
- 3. Broad high nasal root
- 4. Hypoplasia of lateral cartilages of the nose
- 5. Premature greying, predominance of grey scalp hair before age 30.

Other recognize traits that do not contribute to the assignment of phenotype are: spina bifida; cleft lip or palate; Hirschsprung disease; limb defects; congenital heart abnormalities; vestibular defects; low anterior hair line; broad square jaw.

2. Preparation of Genomic DNA.

DNA was obtained from 20 ml of heparinized blood samples. Blood cells were lysed by the addition of an equal volume of 0.1 M Tris-HCl pH7.9, 1 mM EDTA, 20 mM NaCl, 4% SDS. After a 30-min. incubation at room temperature, the lysate was extracted with an equal volume of salt-saturatedphenol (SS-phenol) with shaking for 10 min. Following a 20min. centrifugation at 1.800 g (25°C), the agueous phase was removed and the DNA was precipitated with the addition of 1/10 vol. of 3 M NH₄OAc and 2.5 vol. of 100% ethanol. Samples were again centrifuged 10 min. at 1,800 g (25°C). The DNA was then dissolved in 1.6 ml of 50 mM Tris-HCl pH 7.9, 0.5 M EDTA, 10 mM NaCl. The samples were digested with 9 units RNAase A (Sigma) for 30 min. at 37°C; brought to 0.5% SDS, and digested with 17 units of Pronase (Sigma) for 2 hours at 37°C. Samples were re-extracted with SS-phenol; ethanol precipitated, washed in 70% ethanol, and solubilized in 0.5 ml 10 mM Tris-HCl pH 8.0, 1 mM EDTA, yielding 200-600 μg of high molecular weight DNA.

3. Southern Blots.

Genomic DNA (3-5 μ g) was digested with the appropriate restriction endonucleases and separated by electrophoresis through 0.8% or 2.0% agarose gels. The gels were denatured and neutralized, then blotted by capillary transfer to either Hybond-N nylon (Amersham) or Immobilon-N (Millipore) membranes. DNA was bound to the membranes either by UV

irradiation (if membrane was nylon) or baking at 80°C for 1 hour under vaccuum (if membrane was Immobilon-N). Membranes were prehybridized at $42^{\circ}\text{C} > 4$ hours in 50% formamide, 50 µg sheared salmon sperm DNA/ml, 0.1 M PIPES pH 7.04, 0.1 M NaCl, 0.1% Sarkosyl, 0.1% Ficoll, 0.1% PVP-40 (mol. wt. 360,000), 0.1% BSA. Blots were hybridized > 16 hours 42° C in a solution identical to the prehybridization solution with the exceptions that the formamide concentration was reduced to 40%, the concentration of salmon sperm DNA was reduced by half (25 μ g/ml), and α ³²P-dATP (10 μ Ci/ml) labelled probe was added to a concentration of 1×10^6 CPM/ml. Probes were random primer labelled to a specific activity of $\sim 1 \times 10^9$ according to the method of Feinberg and Vogelstein [21]. Blots were washed in 2x SSC, 0.05% N-laurylsarkosine, 0.02% NaPPi at room temperature followed by two 1-hour washes with 0.1x SSC, 0.05% N-laurylsarkosine, 0.02% NaPPi at 50°C. Blots were exposed to X-ray film for 1-5 days with intensifying screens.

4. PCR Amplifications.

All PCR fragments were amplified from 100 ng of genomic DNA in 50 µl reactions containing 0.25 µM of each primer, 200 µM dNTPs, 2 units Taq polymerase (Boehringer Mannheim), the manufacturer's reaction buffer, and a 50 µl overlay of mineral oil (USB). All reactions were performed in a PTC-100 thermocycler (MJ Research). Fragment identities, primer pairs and conditions for amplification are presented in

Table A2. All samples were denatured at 95°C for 5 min prior to the addition of Taq polymerase, and the final extension time was increased to 5 minutes. Mineral oil was removed from the PCR product by separation on Parafilm M. In the case of PCR amplification of (CA)_n regions for genotyping (CD3D, D11S35, and PAX3 (CA)_n), and amplification for subsequent SSCP analysis, PCR parameters were modified as follows: genomic DNA was amplified for 25 cycles in a 25 μ l volume with 100 μ M dNTPs. This reaction mixture was then supplemented to make a final volume of 50 μ l; 200 μ M dCTP, dTP, dGTP; 50 μ M dATP; and 0.4 μ l ³⁵S-dATP (10mCi/ml). The reaction continued for 10 more cycles.

5. Genotyping for Dinucleotide Repeat Markers.

Six μ l of 35 S-dATP labelled PCR mixture was diluted with 4 μ l of sequencing loading buffer, heated at 95°C for > 5 min., then chilled on wet ice. 1-3 μ l of this mixture was then loaded on 6% polyacrylamide sequencing gels containing 8 M Urea and 12% formamide. A dideoxy labelled M13 sequence was usually run on the same gel in order to estimate allele sizes (assigned according to the darkest band in the set of bands generated for each dinucleotide containing fragment). Samples were electrophoresed for 3-6 hours at 50 Watts (50 C). Gels were fixed in 15% methanol, 10% acetic acid for 45 min., then dried on a slab dryer. Dried gels were exposed to X-ray film for 1 to 10 days at room temperature.

6. SSCP Analysis.

35S-dATP labelled PCR fragments were diluted and denatured as for genotyping as described above. Samples were electrophoresed on 20 x 45 cm native 0.5x MDE Hydrolink gels (AT Biochem) in 0.6x TBE buffer, at 8 Watts for 14 hours at room temperature, or at 12 Watts for 8 hours at 4°C. No substantial difference was seen between the two methods of electrophoresis. Gels were dried on a slab drier without fixing and exposed to X-ray film for 1-10 days.

7. Sequencing.

PAX3 PCR fragments from affected individuals that showed an SSCP, and all PAX3 PCR fragments from the probands of UGM1 and MSU5, were cloned directly into pCR 1000 (Invitrogen). The exon 2 fragments from UGM2-18 were first enriched for the mutant fragment by digestion with RsaI and electrophoresis on 4% NuSeive 3:1 agarose gels (FMC). Following restriction with RsaI, the wild type fragments migrated at 416 bp and 119 bp, while fragments from the mutant allele migrated at 535 bp.

All potential mutant fragments were excised from the gel and eluted using the Geneclean system (Bio 101), and then cloned into pCR 1000 (Invitrogen). Plasmid DNA from clones was isolated using Magic Miniprep (Promega), and then alkali denatured prior to sequencing according to the method of Wang et al.[59]. For each sequencing reaction, 2 µg double stranded plasmid DNA and 6 ng of primer were used in the

Sequenase system v.2 (USB). In all sequencing experiments 3 independent clones were sequenced with primers for both strands. Sequencing primers were the same as those for PCR, with the addition of JA4 and JA5, which prime between the TF30 and TF32 sites in exon 2.

For all detected sequence changes representing potential mutations, a restriction site change was created. That the mutation was not a PCR artifact was then confirmed by digestion of PCR fragments with the appropriate restriction endonuclease. In the case of the 14 bp deletion segregating in UGM2, the existence of the mutation was confirmed by the loss of an Rsa I site in fragments generated from affected individuals. In the case of the 1 bp insertion segregating in MSU3, the existence of the mutation was confirmed by the gain of an Ava I restriction site in fragments generated from affected individuals. A 1 bp substitution that would have created a Tha I site in an allele from MSU5-21 could not be confirmed with Tha I digestion. Subsequent attempts to isolate another clone containing this "missense mutation" were not successful, and it was concluded that the 1 bp substitution was a PCR artifact. The SSCP detected in the unaffected individuals MSU2-6 and MSU5-18 was confirmed to be due to a Hae III polymorphism (described by Baldwin et al.[7]) in the intron 5' to exon 2 by Hae III digestion.

8. Linkage Analysis.

Linkage analyses were performed using the Linkage (v. 5.10) program package kindly supplied by Dr. Jurg Ott, Columbia University Medical School. Full data files for all families are presented below. When affection status was assigned the following parameters were used: a) for WS1 the penetrance for WS1/+ and WS1/WS1 genotypes was 95%; the penetrance for the +/+ genotype (i.e. probability of a phenocopy) was 0.001; gene frequency was 1/42,000. b) for WS2 the penetrance for WS2/+ was 57%, WS2/WS2 was 95% and the penetrance for +/+ was 0.001. The gene frequency was 1/2100. The latter figure is often cited in the literature and attributed to Arias et al.[2]. In fact, no data has ever been presented to support this figure. Arias extrapolated the gene frequency for WS2 from a consideration of the frequency of hereditary white forelock in the population. The overall effect of overestimating the gene frequency in the linkage analysis is to make obligate recombinations involving individuals classified as affected more difficult to detect, and to weaken the overall efficiency.

Table A2. PCR and Sequencing Primers

LOCUS	ID	Sequence (5'-3')	Cycling parameters*
CD3D	TF41	TAGCTGGTGCATAAGCTCAC	94° C 0:45
	TF42	GTTAGTGGAAGAGCAGAGC	55° C 1:00
			72° C 2:00
D11s35	TF39	ACAATTGGATTACTACTAGC	95° C 0:45
	TF40	TGTATTTGTATCGATTAACC	52° C 0:45
			72° C 0:45
PAX3 (CA) _n	TF26	CAGGGAGATGGCAGTT	94°C 0:45
••	TF38	CAGAGGCACAGAAAGA	50° C 1:00
			72° C 1:00
PAX3 Exon1	TF58	CCGTTTCGCCTTCACCTGGA	94° C 0:45
	TF59	GCGCTGAGGCCCTCCCTTAC	60° C 0:45
			72° C 1:00
PAX3 Exon2	TF30	ATTTTGCCCCATTTGCTGTC	94° C 0:45
	TF32	CCGGTCTTCCCCAACACAGG	61° C 0:45
			72° C 1:00
PAX3 Exon3	TF33	CCTGCCCGCCTGTTCTCT	95°C 0:45
	TF34	CGACTGACTGTCGCGCCT	60° C 0:45
			72° C 1:00
PAX3 Exon4	TF35	AGCCCTGCTTGTCTCAACCATGTG	94° C 0:45
	TF36	TGCCCTCCAAGTCACCCAGCAAGT	66° C 0:45
			72° C 0:45
RHO Exon1	TF60	AGCTCAGGCCTTCGCAGCAT	94° C 0:45
	TF61	GAGGGCTTTGGATAACATTG	60° C 1:00
			72° C 0:45
PAX3 Exon2	JA4	CCAACCACATCCGCCACAAG	Sequencing primer
PAX3 Exon2	JA5	ACTGCGAAATTACGTGCTGC	Sequencing primer

^{* =} All PCR reactions for 30 cycles plus a final 5 min. extension.

IV. Appendix B

Additional Figures and Tables

Table B1. MSU4 Linkage Data File

ID#	Father	Mother	Aff.	Sex	PAX3	D11S35	CD3D
1 1	0	0	2	2	64	44	2 5
1 2	0	0	1	1	0 0	0 0	00
1 3	2	1	2	2	64	3 4	23
1 4	0	0	1	1	7 8	2 2	26
1 5	2	1	1	2	74	24	2 2
1 6	0	0	2	1	8 3	2 3	56
1 7	2	1	1	0	64	2 4	2 5
1 8	0	0	2	1	49	2 5	56
1 9	2	1	2	2	44	3 4	23
1 10	0	0	1	1	27	1 2	23
1 11	2	1	1	1	64	3 4	23
1 12	0	0	2	1	74	24	36
1 13	4	3	2	1	47	23	36
1 14	4	3	1	1	76	00	36
1 15	5	6	2	1	7 8	24	26
1 16	5	6	2	1	3 4	3 4	2 5
1 17	7	8	2	0	69	2 2	26
1 18	7	8	1	0	00	2 5	2 5
1 19	10	9	1	1	7.4	23	23
1 20	10	9	1	1	74	24	23
1 21	11	12	1	1	7.4	44	36
1 22	11	12	1	1	7 4	44	26
1 23	11	12	2	1	0 0	0 0	0 0

Aff.: 1 = normal; 2 = affected.

Sex: 1 = male; 2 = female.

PAX3: Dinucleotide marker for locus.
D11s35: Dinucleotide marker for locus.
CD3D: Dinucleotide marker for locus.

Table B2. MSU5 Linkage Data File

			S	A			- 11-					
ID	F	м	E	F	ALPP	D2s3	a/b (x10)	FN1	D2s55	TNP1	PAX3	D2s211
1	0	0	1	1	00	0000	0.00	00	00	00	00	00
2	0	0	2	2	11	0011	7.26	01	11	01	89	22
3	1	2	2	2	11	0010	7.00	01	11	01	59	26
4	1	2	1	2	11	0010	6.94	01	11	01	59	26
5	0	0	1	1	00	0000	0.00	00	00	00	00	00
6	5	3	1	2	10	1010	6.67	01	11	01	49	56
7	5	3	2	2	10	1010	7.26	01	01	01	49	56
8	9	3	1	1	01	1010	5.36	11	11	00	00	66
9	0	0	1	1	01	1100	4.76	11	11	01	44	36
10	0	0	2	1	11	1010	5.45	10	10	00	79	46
11	4	10	1	2	11	1010	7.27	11	11	11	79	26
12	4	10	1	1	01	1010	4.82	11	10	00	57	66
13	4	10	2	1	11	0010	5.00	11	11	11	57	66
14	4	10	1	2	11	1010	7.17	11	10	11	99	24
15	4	10	2	1	01	1010	5.49	11	11	00	57	66
16	0	0	1	1	10	0000	5.38	01	00	01	99	45
17	0	0	2	1	11	0000	5.00	10	00	01	16	47
18	16	17	2	1	11	1010	5.82	11	11	01	69	45
19	0	0	1	1	01	0010	5.22	10	01	11	37	48
20	0	0	2	1	01	0000	4.84	00	10	00	00	56
21	0	0	2	1	11	0101	5.32	10	11	11	45	36
22	0	0	2	1	01	0011	5.00	10	11	01	46	18
23	0	0	1	1	11	0101	4.33	11	10	01	34	36
24	0	0	1	1	11	0110	5.56	10	01	11	99	48
25	6	18	1	2	11	0010	6.78	11	11	01	69	45
26	6	18	1	2	10	1010	6.73	01	10	01	99	56
27	6	18	2	1	10	0010	5.66	01	11	01	00	56
28	19	7	2	1	11	1010	5.00	11	01	11	47	68
29	8	20	1	1	01	0000	5.56	00	00	00	00	66
30	11	21	1	1	01	0000	5.38	00	00	00	00	00
31	11	21	2	2	10	0110	6.85	11	11	01	59	26
32	11	21	2	2	11	0011	7.00	11	11	11	49	23
33	12	22	2	1	01	1001	5.09	11	10	01	47	16
34	12	22	2	1	01	0010	5.56	11	11	01	56	68
35	23	13	1	1	01	0011	5.36	01	11	01	35	66
36	23	13	1	1	01	0011	5.56	01	10	01	00	66
37	23	13	1	2	00	0000	6.00	00	00	00	00	00
38	24	15	2	1	00	0110	5.36	11	01	00	79	68
39	24	15	2	2	11	1010	6.22	10	11	10	79	46

	Table B3. MSU6 Linkage Data File											
ID	F	M	Sex	Aff	ALPP	D2s55	FN1	SAG	a/b (x10)	W	PAX3	W (aff.)
1	0	0	2	1	1 0	1 0	1 1	1 1	5.38	1.75	1 1	1
2	0	0	1	2	1 1	1 1	1 0	1 0	6.46	2.31	5 6	2
3	2	1	2	1	1 1	1 0	1 1	1 1	5.00	1.63	1 6	1
4	0	0	1	1	1 1	1 0	1 0	1 1	5.00	1.63	6 6	1
5	2	1	1	1	1 1	1 0	1 1	1 1	5.64	1.95	1 5	2
6	0	0	2	1	1 0	1 0	1 0	1 1	4.91	1.57	3 6	1
7	2	1	2	2	1 0	1 0	1 0	1 1	5.61	1.87	1 5	2
8	0	0	1	1	1 1	1 0	1 1	1 1	4.84	1.59	1 6	1
9	2	1	1	2	1 1	1 1	1 0	1 1	6.32	0.00	1 6	2
10	0	0	2	1	1 0	0 1	1 1	1 0	5.83	2.05	1 4	2
11	2	1	1	1	1 1	1 1	1 0	1 1	4.59	1.46	1 5	1
12	2	1	2	1	1 1	1 1	1 1	1 1	5.18	1.69	1 5	1
13	0	0	1	1	1 1	1 0	1 1	1 0	5.08	1.66	2 6	1
14	2	1	2	2	1 1	1 0	1 1	1 0	5.35	1.69	1 6	1
15	4	3	2	1	1 0	1 0	1 1	0 1	5.00	1.58	1 6	1
16	5	6	2	1	1 1	1 0	1 1	0 0	5.45	1.80	1 6	1
17	5	6	1	2	1 1	1 0	1 1	1 1	5.09	1.66	1 3	1
18	8	7	1	2	1 1	1 0	1 0	1 0	5.09	1.67	5 6	1
19	8	7	1	2	1 0	1 0	1 1	1 1	5.21	1.66	1 5	1
20	9	10	2	2	1 1	1 1	1 1	1 1	6.53	2.22	1 1	2
21	13	12	1	1	1 1	1 1	1 1	1 0	5.83	1.97	5 6	2

		T	able B4.	UGM1 I	Linkage	Data Fi	le		
ID	P	M	Sex	Aff.	a/b	D2s55	ALPP	TNP1	PAX3
6	0	0	2	2	0.00	0 0	0 0	0 0	0 0
7	0	0	1	1	5.08	1 1	1 1	0 1	9 9
28	0	0	1	1	6.77	1 0	1 0	0 1	9 9
29	7	6	2	2	6.52	1 1	1 1	0 0	5 9
30	7	6	2	2	6.31	1 0	1 0	1 1	5 9
31	0	0	1	1	5.50	1 1	1 0	1 1	9 9
32	7	6	2	1	5.00	1 1	1 1	1 1	2 9
33	0	0	1	1	5.23	1 0	1 1	0 0	3 9
34	7	6	1	1	5.65	1 1	0 1	1 1	2 9
35	0	0	2	1	5.57	1 1	1 1	1 1	3 9
63	28	29	1	1	5.52	1 0	1 0	0 1	9 9
64	28	29	1	2	7.10	1 0	1 0	0 0	5 9
65	28	29	2	2	7.30	1 0	1 0	1 1	5 9
66	31	30	2	2	7.14	1 0	1 0	1 0	5 9
67	31	30	1	2	6.51	1 0	1 0	1 0	5 9
68	31	30	1	2	6.88	1 1	1 0	1 0	5 9
69	33	32	2	1	5.67	1 1	1 0	0 0	2 3
70	33	32	1	1	5.41	1 1	1 0	0 1	9 9
71	33	32	1	1	5.67	1 0	1 1	0 0	2 9
72	34	35	1	1	5.15	0 1	1 1	1 1	3 9
73	34	35	2	1	5.90	1 1	1 1	1 0	2 9
74	34	35	1	1	5.93	0 1	1 1	1 1	3 9
75	34	35	2	1	5.79	1 1	0 1	1 1	9 9
76	34	35	2	1	0.00	0 0	0 0	0 0	0 0

1 2 3 4 5 6 7 8 9 10 11 12 13 14 15 16 17 18 19 20 21

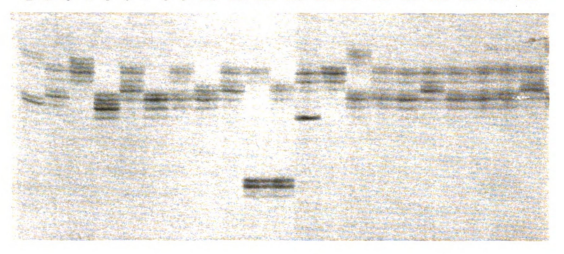


Figure B1. MSU4 PAX3 Ge1.

Dinucleotide repeat of PAX3 PCR amplified from members of family MSU4. Lanes 1-21 correspond to individuals MSU4-1 through MSU4-21. Assigned genotypes are given in Table B1. PCR amplification parameters are given in Table A2.

1 2 3 4 5 6 7 8 9 10 11 12 13 14 15 16 17 18 19 20 21

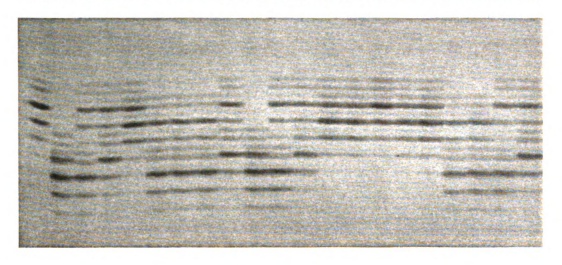


Figure B2. MSU4 CD3D Gel.

Dinucleotide repeat of CD3D PCR amplified from members of family MSU4. Lanes 1-21 correspond to individuals MSU4-1 through MSU4-21. Assigned genotypes are given in Table B1. PCR amplification parameters are given in Table A2.

1 2 3 4 5 6 7 8 9 10 11 12 13 14 15 16 17 18 19 20 21

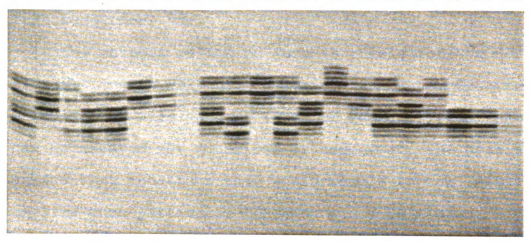


Figure B3. MSU4 D11S35 Gel.

Dinucleotide repeat of D11S35 PCR amplified from members of family MSU4. Lanes 1-21 correspond to individuals MSU4-1 through MSU4-21. Assigned genotypes are given in Table B1. PCR amplification parameters are given in Table A2.

V. Appendix C

Detection of Changes in Copy Number at Regions of Candidate
Loci By Dot Blot Analysis

1.Introduction

The methods relied on in this thesis for the detection of mutations in PAX3 have a serious weakness. Because fragments of alleles must first be PCR amplified before they can be assayed for mutations or sequenced, the possibility exists that mutations that would result in the inability to amplify that particular fragment would be missed. A mutation in the primer target sequence, or various size deletions, could result in inability to amplify the mutant allele, with the consequence of false identification of a +/(del) set of fragments as being +/+. This type of error has been demonstrated before by Fujimura et al.[24] and more recently by Beutler et al.[11]. While any PCR-based method of detection of alleles has this limitation, it is particularly important to recognize this potential source of error in detecting WS mutations because deletions and null alleles have been demonstrated to give rise to the WS and Sp phenotypes.

Accordingly, all of the probands of the WS families in this study were assayed for changes in copy number at PAX3 and for markers from the 3p and 3q candidate regions [4]. Two methods were chosen. First, Southern blots of EcoRI digested genomic DNA were probed with PAX3 (exon 2) probes that had

been $\alpha^{-32}\text{P-dATP}$ random primer labelled. No fragments of unusual length were detected with this method. Since this method would only detect deletions that removed part, but not all, of sequences within a restriction fragment or changes at the restriction site itself, it was decided to be too inefficient to continue. Changes in copy number were then assayed for by hybridization of probes to genomic dot blots. The results of these experiments are summarized below.

2. Results

Initially, dot blots were made using nitrocellulose filters (Schleicher and Schuell). The methods were as follows:

- a) Genomic DNA from each proband of the WS families was used for analysis, with the exceptions of MSU6 in which case DNA of both of the parents were used and MSU4 where DNA from the severely affected individual MSU4-25 was included. DNA from a randomly selected individual (HK27) was included as a normal control. The characteristics, race, and sex of this individual are not known.
- b) 2 μ g of DNA was diluted with TLE to make a final volume of 10 μ l. The sample was boiled for 5 min., then chilled on wet ice.
- c) 40 μ l of chilled 20x SSC was added to each sample.
- d) A nitrocellulose filter was pre-wetted with 10x SSC, and placed in a dot blot apparatus (Schleicher and Schuell) over 2 Whatman filter papers which were soaked in 10x SSC.
- e) Wells were rinsed with 200 μl of chilled 20x SSC.
- f) Samples were added under vacuum.
- Wells were rinsed again with 200 μ l of chilled 20x SSC.

- h) The filter was UV crosslinked in a Stratalinker (Stratagene) while damp and allowed to air dry for at least 3 hours.
- i) Filters were probed and washed exactly as for Southern blots. Probes were made for PAX3 using PCR fragments including exon 2 (primers TF30-TF32) exon 3 (TF33-TF34) and exon 4 (TF35-36); a murine genomic clone Erba-2 which should hybridize to the homologous sequence THRB on human 3p21; a murine cDNA clone of Rho (MOPS-M2) which should hybridize to the RHO locus on human 3q21-24; a human cDNA clone for carbonic anhydrase II gene located on 8q.
- j) Filters were exposed to a phosphor plate for 12 to 18 hours, and the plate was then scanned on a PhosphorImager (Molecular Dynamics). The signals were quantified and comparisons made using the ImageQuant software system (Molecular Dynamics).
- k) Filters were stripped with three 15 min. washes of boiling 0.1x SSC/0.1% SDS. Filters were then exposed to autorad film for > 5 hours to confirm they had been adequately stripped of probe before being reprobed.

Three dot blots totalling 5 repetitions of each sample were analyzed. The data from the first blot was discarded due to the ommission of the normal control (HK27) from that blot. All pair-wise comparisons between total counts for probes were first normalized to the HK27 ratio in each series, and then averaged over the four repetitions for each sample. The results of comparisons from the 4 series are summarized in the following tables.

Table C1. Ratios of PAX3 exon Copy Numbers to Other Loci

То	to Erba	2	Tota	l ratios to	Rho	Total ratios to CarbII			
id#	Exon2	Exon3	Exon4	Exon2	Exon3	Exon4	Exon2	Exon3	Exon4
msu1-3	0.806	1.964	1.669	1.383	2.2	2.384	0.993		1.934
msu2-7	0.929	1.804	2.01	0.903	1.687	2.441	0.906		1.938
msu3-9	1.01	0.921	1.127	1.167	0.961	1.37	1.153		1.289
msu4-4	0.844	0.942	0.914	1.253	1.412	1.363	0.838		0.855
msu4-25	0.861	0.885	0.808	0.88	0.939	0.86	0.857		0.82
msu5-21	0.94	1.684	0.85	1.032	1.339	1.048	0.953		0.92
msu6-54	0.879	0.665	0.671	0.83	0.829	0.634	0.822		0.608
msu6-55	0.889	1.05	0.802	0.898	0.923	0.815	0.878		0.782
msu7-6	0.975	1.143	1.135	1.316	1.622	1.626	1.443		1.69
msu9-c	0.96	2.371	1.343	1.328	2.264	1.821	1.057		1.35
ugm1-66	0.622	0.894	0.659	1.12	1.564	1.232	0.593		0.628
ugm2-24	0.947	1.136	0.895	0.97	1.289	0.928	0.966		0.874
ugm3-11	1.076	1.541	1.02	1.123	1.514	1.156	1.131		1.121
ugm4-10	0.879	0.983	0.794	1.044	1.205	0.955	0.916		0.865
ugm5-1	0.986	0.874	0.909	1.204	1.325	1.083	0.966		0.903
HK27	1.002	1	1	1	1	1	0.999		1

There are significant deviations from 1:1 ratios represented in the table. The most prominent are highlighted. The greatest deviations are invariably seen with the exon 3 probe. However, the standard deviations within series are also highest with this probe -- typically ~0.5 or higher while standard deviations within series with the exon 2 probe are ~0.2. This is probably due to the high proportion of paired domain sequence in the exon 3 probe while the exon2 probe has nearly 50% intronic sequence. Thus, the exon 3 probe may be hybridizing to several PAX genes. For this reason, the exon 3:CA2 comparisons were not even made.

If one discounts the data for the exon 3 probe then it appears that individuals MSU1-3 and MSU2-7 have duplications

for exon 4 (the exon 4 probe also has a high proportion of unique sequence and standard deviations in the series comparable to the exon 2 probe); individual MSU6-54 appears to have a deletion of PAX3; and individual UGM1-66 appears to have a deletion of PAX3 when compared to the Erba-2 and CA2 probes, but not when compared to the Rho probe. A resolution to the latter contradiction is suggested by pairwise comparisons of the non-PAX3 probes.

Table C2. Ratios of Non-PAX3 Loci Comparisons

	CA2	Ærba2	CA	2/Rho	Rho/Erba2		
id#	avg	stdev	avg	stdev	avg	stdev	
msu1-3	0.9	0.255	1.42	0.35	0.67	0.24	
msu2-7	1.08	0.187	1.16	0.26	0.95	0.23	
msu3-9	0.89	0.128	1.06	0.3	0.89	0.25	
msu4-4	1.05	0.184	1.62	0.24	0.66	0.08	
msu4-25	0.98	0.181	1.02	0.13	0.98	0.26	
msu5-21	0.99	0.185	1.09	0.24	0.97	0.34	
msu6-54	1.08	0.204	1.04	0.26	1.13	0.48	
msu6-55	1.02	0.079	1.06	0.12	0.98	0.15	
msu7-6	0.75	0.266	0.95	0.08	0.78	0.24	
msu9-c	0.95	0.22	1.29	0.23	0.77	0.24	
ugm1-66	1.03	0.069	1.97	0.33	0.54	0.09	
ugm2-24	1.02	0.078	1.1	0.18	0.95	0.15	
ugm3-11	0.96	0.162	1.03	0.15	0.96	0.22	
ugm4-10	0.94	0.119	1.16	0.12	0.82	0.1	
ugm5-1	1	0.127	1.27	0.23	0.83	0.27	
hk27	1	7E-05	1.01	0.01	1	0	

All of the ratios are consistently near 1:1 with the notable exceptions of those that are highlighted. In particular, individuals MSU1-3, MSU4-4 and UGM1-66 appear to have reduced copies of RHO, which may be indicative of a

deletion on 3q. Pairwise T-test comparisons of the measures of these three samples with the other samples gave evidence of significant differences (p = 0.0016). A deletion encompassing RHO would explain why the PAX3:RHO ratios were 1:1 for UGM1-66 (assuming that UGM1-66 has a deletion of PAX3 as well) and why the PAX3:RHO ratio was exceptionally high in MSU1-3 (assuming that MSU1-3 has a duplication of PAX3). Potentially the most interesting observation is that MSU4-4 may have a deletion of RHO and no obvious change in copy number at PAX3. MSU4 is segregating for WS2, and linkage analysis detected an obligate recombination between WS2 and the PAX3 dinucleotide marker (see Chapter 1). These observations suggested that there may be another locus for the WS phenotype on 3q which serves to modify the WS1 phenotype and may be sufficient to cause the WS2 phenotype.

At first, the coincidence of perhaps three individuals (MSU1-3, MSU2-7, UGM1-66) in a sample of 15 having changes of copy number at both the 2q and 3q regions may seem too unlikely. However, it should be remembered that the families analyzed were chosen precisely because they presented obvious phenotypes. If a major modifying locus of WS1 is located on 3q, it is in the most obviously affected individuals that mutations would be expected at both loci. In other words, the sample set may be biased towards finding coincident mutations. Also, it is possible that the deletions and duplications of 2q and 3q are causally

related, perhaps by non-homologous recombination during meiosis.

In order to confirm these conclusions, the experiments were repeated on a dot blot containing DNA from all of the members of UGM1 to test for Mendelian inheritance of the deletion, and correspondance to phenotype. Ideally, this analysis would have been repeated for families MSU4 and MSU6, but the uncertainties regarding the phenotypes in these families (see Chapter 1) render dubious any conclusions from such analyses.

When ratios of PAX3 to Erba-2 were compared in UGM1, it was observed that not only did the apparent deletions not correspond 1:1 with the WS1 phenotype, but the deletions did not segregate in Mendelian fashion. Because of this observation, and the high standard deviations in some of the other samples on the original dot blots, it was decided that all experiments should be repeated with modifications designed to make each experiment more reproducible.

Numerous changes in the procedure were tried. Instead of presenting the results with each modification, I will summarize all of the modifications that I believe were useful.

a) Dot blots were made using Hybond-N nylon membranes (Amersham). This allowed probes to be removed using a 30 min. wash with 0.4 N NaOH. Probe removal was uniform and complete at each step, which was not true of the boiling SDS procedure used with the nitrocellulose filters.

- b) A PCR fragment of exon 1 of the human RHO gene was substituted for the murine Rho probe. This allowed for more comparable hybridization kinetics to the PAX3 probe both because it contains human sequence and because the probe lengths are similar (535 bp vs. 585 bp).
- c) A different hybridization solution was used which contains no salmon sperm DNA. Hybridization solution is 37% formamide; 1% SDS; 10% dextran sulfate; and 5x SSPE. 15 mls. of this was used as a pre-hyb. The pre-hyb was then substituted with a 15 ml. solution containing probe. The absence of salmon sperm DNA allows for careful control of the ratio of probe DNA to target DNA, which will affect the kinetics of hybridization. Unless linear kinetics are achieved, it will not be possible to reliably detect changes in copy number.
- d) Six normal control samples were substituted for the one HK27 control sample. They were MSU5-19, MSU5-18, MSU5-21, MSU5-22, UGM2-22 and UGM2-41. These samples have the advantage that the individuals have all been inspected and determined to be clinically normal. They all have married into the respective families and have no family history of WS themselves. By using the average measurements for these six as the normalizing factor an error of compounding variation is removed from the analysis. There may be variation between repetitions of samples that are due purely to the limitations of the technique. By normalizing a test sample to a control sample that itself is subject to those inherent variations the overall variation is compounded. By normalizing to an average of control samples, the only source of variation should be in the test samples. In fact, the standard deviations within series did improve with this technique.
- e) A Southern blot should be included in the hybridization chamber with each dot blot to confirm that any signal detected is due to specific hybridization to a discrete sequence, and as a rough estimation of the number of sequences in the genome that the probe is hybridizing to.

- f) The probes for CA2, Erba-2, and exon 3 of PAX3 should be discontinued to minimize the number of hybridization and stripping steps for each blot. Matched sets of blots should be probed with RHO, and PAX3 exon 2, and an X-linked marker in scrambled order.
- g) A unique sequence X-linked marker should be used to first determine whether males and females can be distinguished with the technique. The DXs14 marker was tried but is not suitable since it recognizes many bands (>15) on a Southern blot and gives exceptionally high background signals on dot blots.
- h) The total amount of probe in the hybridization solution should be calculated to give at least a ten-fold excess of probe per ml to target sequence. If you assume that the target sequence is approximately 10³bp in length, then it represents $10^3/10^9$ of the total sequence. Thus, the total amount of genomic DNA on a blot should be divided by 10⁶, and this figure multiplied by 10 to give the total amount of probe in solution. For example: if a blot contains 160 μ g of genomic DNA, then the probe should contain ten times 0.16 ng of DNA per ml, or 16 ng in a 10 ml hybridization solution. For several experiments I added labelled probe up to 2 x 10⁶ CPM/ml and then supplemented the total with unlabelled probe to achieve 20 ng/ml. I now regard this as a mistake since this meant having 4 to 5 times as much unlabelled probe as labelled probe in solution. Since kinetics of solution hybridization are favored over hybridization to a 2 dimensional matrix, linear kinetics with regard to the target sequences on the membrane was probably not achieved. The hybridization solution should contain only labelled probe fragments, with no other DNA in solution.

Analysis with the above modifications had to be terminated due to time constraints and the unexpected characteristics of the DXs14 probe. Once a suitable X-linked probe is found, I feel confident that male to female differences can be detected with the dot blot method. The initial observations can then be reliably tested.

If the original changes in copy number are confirmed, but the deletion of PAX3 shows non-Mendelian segregation in UGM1, I would strongly urge that the entire UGM1 sample set be typed for a group of highly polymorphic markers not linked to 2q. A possible resolution of the non-Mendelian inheritance pattern originally seen would be if several DNA samples were mislabelled. It should be pointed out that the Mendelian pattern of inheritance observed with the PAX3 marker may be coincidental, or may be a reflection of the tendency for this observer to assume that the pedigree structure and sample labels are all correct and to resolve ambiguous genotype assignments in favor of Mendelian inheritance.

If the original observations cannot be repeated with the modification of the dot blot method described here, my suggestion would be to attempt to show changes in copy number with in situ hybridization techniques. It is possible, however, that the original observations were due to inconsistencies inherent in the methodology. Given the reproducibility of the UGM1-66 data, there may be a component of the DNA sample that renders it prone to removal from a nitrocellulose filter by the boiling SDS method.

VI. Appendix D

Conventions of Nomenclature for Human Alleles Used in this Thesis

The allele designations used in this thesis are a modification of McKusick [45]. The goal is to develop a short-hand method for referring to particular mutations while still conveying as much information as possible about the mutation.

Allele designations follow the locus name in brackets {}. The field inside the bracket should be thought of as having a center, where the codon involved in the mutation is located, and fields to the left and right. The field to the left is reserved for either a description of the nucleotide change or the identity of the codon in the normal allele. The field to the right is reserved for either a description of the new translation codon or the identity of the codon after the mutation. Certain symbols for deletions, insertions, etc. should be agreed upon for the sake of brevity. I propose:

 $\Delta =$ deletion

 ∇ = insertion

FS = frame shift

TER = new translation termination codon

The alleles are named according to the type of mutation and the functional consequence on the predicted translation product. All mutations are numbered in reference to the codon number in the predicted reading frame. Thus, a missense mutation in PAX3 that results in a Leucine for Arginine substitution at position 50 is designated: PAX3{Arq50Leu}. A 1 base pair insertion that causes a shift in the reading frame, and early translation termination resulting in a peptide 113 amino acids in length would be designated: PAX3{1bp ∇ 34;FS113TER}. For ease of reference, I suggest that the translation termination codon be numbered in reference to the position in the mutant allele. The new translation termination codon in the 14 bp deletion mutant allele straddles 112 and 113 codons in the wild-type allele, but is unambiguously defined as the 108 codon in the mutant allele (PAX3{14bp Δ 89-93;FS108TER}).

Modifications of the system are needed to account for more complex mutations such as tri-nucleotide repeat expansions or splice site mutations, especially when such mutations involve nucleotides in non-coding regions. When deciding on an allele designation it should be remembered that the goal is to achieve a unique, short, and readily idetifiable name and not a full description of the molecular pathology. The intronic mutation in Pax-3 that results in at least four aberrant splicing products (Sp) is a case in point [19]. Instead of attempting to describe each translated product it may be sufficient to simply indicate that a

nucleotide change in intron 3 results in aberrant splicing. Perhaps PAX3{I3splice} would suffice (if this were a human mutation)?

VII. Appendix E

Results of Linkage Analysis for Mi^{OR}

1. Introduction

Asher and Friedman [4] identified several mouse mutations that could be the murine homologs of Waardenburg syndrome. As a positional cloning strategy, they argued that the identification and cloning of the murine gene first would greatly facilitate the cloning of the human gene given the advantages of mapping and cloning a gene from an inbred experimental animal. The murine gene MiOR was the strongest of the candidate genes arguing strictly from phenotypic characters since hearing impairment had been demonstrated in Mi^{OR}/+ animals (J. Asher, unpublished observations), whereas no such impairment had been demonstrated for the other mouse models, including Sp[53]. Unfortunately, the Mi^{OR} model predicted two different human locations based on conserved syntenies between the murine and human genetic maps, depending on whether Mi^{OR} mapped closer to the genes Raf-1 or Rho. Given the relative paucity of informative genetic markers available for the human genome at the time, an efficient strategy was to better resolve the murine map and then concentrate on conducting a multi-locus analysis[38] in the human candidate region which appeared more likely based on the higher resolution murine map. The time and effort expenditure in conducting a multi-locus analysis was considerable, and necessary given the poor informativeness

of the human map, which was composed almost entirely of RFLP and VNTR markers in 1990. A multilocus strategy was necessary in initially demonstrating linkage of WS1 to 2q37 [3].

An interspecific cross was initiated where the Mi^{OR} gene was crossed on to a Robertsonian (4;6) chromosome originating from Mus poschianus. (The original purpose of locating the Mi^{OR} gene on a Robertsonian chromosome was to aid in flow sorting the chromosome should that prove necessary.) This chromosome was then crossed into a Mus musculus line. $Mi^{OR}/+ \times +/+$ crosses were then made, and the progeny typed for white belly spots as a marker for Mi^{OR} , and genotyped for a variety of RFLP markers including Raf-1, Rho, and Try-1.

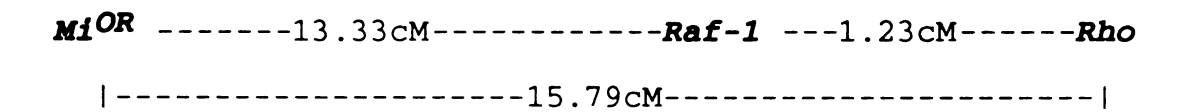
2. Results and Discussion

Genotyping data from Southern blot analysis was coded in a format for use by the Gene-Link program, which was the generous gift of Dr. Xavier Montagutelli, Institut Pasteur, Paris, France. Gene-link calculates liklihood scores, identifies obligate recombinant animals, and double recombinations, and determines confidence levels for the most likely linkage orders.

Table E1. Linkage results for $Mi^{OR}/+ x +/+$

Comparison	Recombinants/N	Distance (cM)
Mi ^{OR} - Raf-1	18/94	19.15
Mi ^{OR} - Rho	16/81	19.75
Raf-1 - Rho	1/81	1.23

Of the 18 recombinants with respect to $Mi^{OR} - Raf-1$, 12 were classified as +/+ and 6 as $Mi^{OR}/+$. Moreover, when considering all markers typed (Raf-1, Mi^{OR} , Rho, Try-1, Met), there are 7 animals in which the only recombination is at Mi; 6 are classified as +/+ and 1 as $Mi^{OR}/+$. Since nonpenetrance for the Mi^{OR} phenotype must be a consideration the analysis was performed considering only those animals with a positive assignment as $Mi^{OR}/+$. The resulting map is:



This linkage order is 100x more likely than the next most likely linkage relationship. Other markers cannot be unambiguously added to the map due to distortion in the map nearer to the centromere, presumably due to the nature of the Robertsonian chromosome.

LIST OF REFERENCES

- 1. Arias, S. "Genetic heterogeneity in the Waardenburg syndrome." Birth Defects Original Article Series (VII): 87-101, 1971.
- 2. Arias, S. and M. Mota. "Apparent non-penetrance for dystopia in Waardenburg syndrome type I, with some hints on the diagnosis of dystopia canthorum." J. Genet. Hum. 26: 103-131, 1978.
- 3. Asher, J. H., Jr., R. Morell and T. B. Friedman. "Waardenburg syndrome (WS): The analysis of a single family with a WS1 mutation showing linkage to RFLP markers on human chromosome 2q." Am. J. Hum. Genet. 48: 43-52, 1991.
- 4. Asher, J. H., Jr., and T. B. Friedman. "Mouse and hamster mutants as models for Waardenburg syndromes in humans." J. Med. Genet. **27**: 618-626, 1990.
- 5. Auerbach, R. "Analysis of the developmental effects of a lethal mutation in the house mouse." J. Exp. Zool. 127: 305-329, 1954.
- 6. Badner, J. A. and A. Chakravarti. "Waardenburg syndrome and Hirschsprung disease: Evidence for pleiotropic effects of a single dominant gene." Am. J. Med. Genet. **35**: 100-104, 1990.
- 7. Baldwin, C. T., C. F. Hoth, J. A. Amos, E. O. da Silva and A. Milunsky. "An exonic mutation in the *HuP2* paired domain gene causes Waardenburg's syndrome." Nature. **355**: 637-638, 1992.
- 8. Balling, R., U. Deutsch and P. Gruss. "undulated, a mutation affecting the development of the mouse skeleton, has a point mutation in the paired box of Pax-1." Cell. 55: 531-535, 1988.
- 9. Bard, L. A. "Heterogeneity in Waardenburg's syndrome." Arch. Ophthal. **96**(2): 1193-1198, 1978.
- 10. Beechey, C. V. and A. G. Searle. "Mutations at the Splocus." Mouse News Lett. 75: 28, 1986.
- 11. Beutler, E., T. Gelbart and C. West. "Identification of six new Gaucher disease mutations." Genomics. 15: 203-205, 1993.

- 12. Bopp, D., E. Jamet, S. Baumgartner, M. Burri and M. Noll. "Isolation of two tissue-specific *Drosophila* paired box genes Pox meso and Pox neuro." EMBO J. 8: 3445-3457, 1986.
- 13. Brown, K. S., D. R. Bergsma and M. V. Barrow. "Animal models of Pigment and hearing abnormalities in man." Birth Defects: Original Article Series (VII): 102-109, 1971.
- 14. Burri, M., Y. Tromvoukis, D. Bopp, G. Frigerio and M. Noll. "Conservation of the paired domain in metazoans and its structure in three isolated human genes." EMBO J. 8(4): 1183-1190, 1989.
- 15. Chalepakis, G., R. Fritsch, H. Fickenscher, U. Deutsch, M. Goulding and P. Gruss. "The molecular basis of the undulated/pax-1 mutation." Cell. **66**: 873-884, 1991.
- 16. Cotterman, C. W. "Some statistical problems posed by Waardenburg's data on dystopia canthorum and associated anomalies." Am. J. Hum. Genet. 3: 254-266, 1951.
- 17. Darwin, C. "The Origin of Species." 1859 London.
- 18. Epstein, D. J., M. Vekemans and P. Gros. "Splotch (Sp^{2H}), a mutation affecting development of the mouse neural tube, shows a deletion within the paired homeodomain of Pax-3." Cell. **67**: 767-774, 1991.
- 19. Epstein, D. J., K. J. Vogan, D. G. Trasler and P. Gros. "A mutation with intron 3 of the *Pax-3* gene produces aberrantly spliced mRNA transcripts in the splotch (*Sp*) mouse mutant." Proc. Natl. Acad. Sci. USA. **90**: 532-536, 1993.
- 20. Farrer, L. A., K. M. Grundfast, J. Amos, K. S. Arnos, J. H. Asher, Jr., P. Beighton, S. R. Diehl, J. Fex, C. Foy, T. B. Friedman, J. Greenberg, C. Hoth, M. Marazita, A. Milunsky, R. Morell, W. Nance, V. Newton, R. Ramesar, T. San Agustin, J. Skare, C. Steven, R. G. J. Wagner, E. R. Wilcox, I. Winship and A. P. Read. "Waardenburg syndrome (WS) type 1 is caused by defects at multiple loci, one of which is near ALPP on chromosome 2: First report of the WS consortium." Am. J. Hum. Genet. 50: 902-913, 1992.
- 21. Feinberg, A. P. and B. Vogelstein. "A technique for radiolabeling DNA restriction endonuclease fragments to high specific activity." Anal. Biochem. 132: 266-267, 1983.

- 22. Foy, C., V. Newton, D. Wellesley, R. Harris and A. P. Read. "Assignment of the locus for Waardenburg syndrome type I to human chromosome 2q37 and possible homology to the splotch mouse." Am. J. Hum. Genet. **46**: 1017-1023, 1990.
- 23. Fraser, G. R. "The Causes of Profound Deafness in Childhood." 1976 Johns Hopkins University Press. Baltimore.
- 24. Fujimura, F. K., H. Northrup and A. L. Beaudet. "Genotyping errors with the polymerase chain reaction." N. Engl. J. Med. 322: 61, 1990.
- 25. Goldberg, M. F. "Waardenburg's syndrome with fundus and other anomalies." Arch. Ophthal. 76: 797-810, 1966.
- 26. Goodman, R. M., G. Oelsner, M. Berkenstadt and D. Admon. "Absence of vagina and right-sided adnexa uteri in the Waardenburg syndrome: a possible clue to the embryological defect." J. Med. Genet. **25**: 355-357, 1988.
- 27. Goulding, M. D., G. Chalepakis, U. Deutsch, J. R. Erselius and P. Gruss. "Pax-3, a novel murine DNA binding protein expressed during early neurogenesis." EMBO J. 10(5): 1135-1147, 1991.
- 28. Gruss, P. and C. Walther. "Pax in development." Cell. **69**: 719-722, 1992.
- 29. Hageman, M. J. and J. W. Delleman. "Heterogeneity in Waardenburg syndrome." Am. J. Hum. Genet. **29:** 468-485, 1977.
- 30. Hayashi, S. and M. P. Scott. "What determines the specificity of action of Drosophila homeodomain proteins?" Cell. **63**: 883-894, 1990.
- 31. Hill, R. E., J. Favor, B. L. M. Hogan, G. F. Saunders, I. M. Hanson, J. Prosser, T. Jordan, N. D. Hastie and V. van Heyningen. "Mouse *Small eye* results from mutations in a paired-like homeobox-containing gene." Nature. **354**: 522-525, 1991.
- 32. Hoth, C. F., A. Milunsky, N. Lipsky, R. Sheffer, S. K. Clarren and C. T. Baldwin. "Mutations in the paired domain of the human PAX3 gene cause Klein-Waardneburg syndrome (WSIII) as well as Waardenburg syndrome type I (WSI)." Am. J. Hum. Genet. **52**: 455-462, 1993.
- 33. Ishikiriyama, S., H. Tonoki, Y. Shibuya, S. Chin, N. Harada, K. Abe and N. Niikawa. "Waardenburg syndrome type I

- in a child with de novo inversion (2)(q35q37.3)." Am. J. Med. Genet. **33**: 505-507, 1989.
- 34. Jacobs-Cohen, R. J., R. F. Payette, M. D. Gershon and T. P. Rothman. "Inability of neural crest cells to colonize the presumptive aganglionic bowel of *ls/ls* mutant mice: Requirements for a permissive microenvironment." J. Comp. Neurol. **255**: 425-438, 1987.
- 35. Kaplan, P. and J.-P. de Chaderevian. "Piebaldism-Waardenburg syndrome: Histopathologic evidence for a neural crest syndrome." Am. J. Med. Genet. 31: 679-688, 1988.
- 36. Lane, P. W. and H. M. Liu. "Association of megacolon with a new dominant spotting gene (*Dom*) in the mouse." J. Hered. **75**: 435-439, 1984.
- 37. Lange, K., M. A. Spence and M. B. Frank. "Application of the lod method to the detection of linkage between a quantitative trait and a qualitative marker: a simulation experiment." Am. J. Hum. Genet. 28: 167-173, 1976.
- 38. Lathrop, G. M., J. M. Lalouel, C. Julier and J. Ott. "Strategies for multilocus linkage analysis in humans." Proc. Natl. Acad. Sci. USA. **81**: 3443-3446, 1984.
- 39. Litt, M., V. Sharma and J. A. Luty. "A highly polymorphic (TG)n microsatellite at the D11s35 locus." Cytogenet. Cell Genet. **51**: 1034, 1990.
- 40. Lyon, M. F. and A. G. Searle. "Genetic Variants and Strains of the Laboratory Mouse." 1989 Oxford University Press. Oxford.
- 41. Mallory, S. B., E. Wiener and J. J. Nordlund.
 "Waardenburg's syndrome with Hirschsprung's disease: A
 neural crest defect." Pediat. Dermat. 3(2): 119-124, 1986.
- 42. Martin, D., N. K. Spurr and J. Trowsdale. "RFLP of the human placental alkaline phosphatase gene (PLAP)." Nucleic Acids Res. 15: 9104, 1987.
- 43. Mayer, T. C. "Site of gene action in *steel* mice: analysis of the pigment defect by mesoderm -- ectoderm recombinations." J. Exp. Zool. **184**: 345-352, 1973.
- 44. McKusick, V. A. "Congenital deafness and Hirshsprung's disease (letter)." New Eng. J. Med. 288: 691, 1973.

- 45. McKusick, V. A. "Mendelian Inheritance in Man." 1988 Johns Hopkins University Press. Baltimore.
- 46. Moase, C. and D. Trasler. "N-CAM alterations in splotch neural tube defect mouse embryos." Development. 113: 1049-1058, 1991.
- 47. Morell, R., T. B. Friedman, S. Moeljopawiro, Hartono, Soewito and J. H. Asher, Jr. "A frameshift mutation in the HuP2 paired domain of the probable human homolog of murine Pax-3 is responsible for Waardenburg syndrome type 1 in an Indonesian family." Human molec. Genet. 1(4): 243-247, 1992.
- 48. Nadeau, J. H. "Maps of linkage and synteny homologies between mouse and man." Trends Genet. 5: 82-86, 1989.
- 49. Perris, R. and M. Bronner-Fraser. "Recent advances in defining the role of the extracellular matrix in neural crest development." Comm. Dev. Neurobiol. 1: 61-83, 1989.
- 50. Pierpoint, J. W. and R. P. Erickson. "Facts on PAX." Am. J. Hum. Genet. **52**: 451-454, 1993.
- 51. Shah, K. N., S. J. Dalal, M. P. Desai, P. N. Sheth, N. C. Joshi and L. M. Ambani. "White Forelock, pigmentary disorder of irides, and long segment Hirshsprung disease: possible variant of Waardenburg syndrome." J. Pediat. 99: 432-435, 1981.
- 52. Sheffer, R. and J. Zlotogora. "Autosomal dominiant inheritance of Klein-Waardenburg syndrome." Am. J. Med. Genet. 42: 320-322, 1992.
- 53. Steel, K. and R. J. H. Smith. "Normal hearing in splotch (Sp/+), the mouse homolog of Waardenburg syndrome type I." Nature Genet. 2: 75-79, 1992.
- 54. Tassabehji, M., A. P. Read, V. E. Newton, R. Harris, R. Balling, P. Gruss and T. Strachan. "Waardenburg's syndrome patients have mutations in the human homologue of the *Pax-3* paired box gene." Nature. **355**: 635-636, 1992.
- 55. Tassabehji, M., A. P. Read, V. E. Newton, M. Patton, P. Gruss, R. Harris and T. Strachan. "Mutations in the PAX3 gene causing Waardenburg syndrome type 1 and type 2." Nature Genetics. 3: 26-30, 1993.
- 56. Ton, C. C. T., H. Hirvonen, H. Miwa, M. M. Weil, P. Monaghan, T. Jordan, V. van Heyningen, N. D. Hastie, H.

- Meijers-Heijboer, M. Drechsler, B. Royer-Pokora, F. Collins, A. Swaroop, L. C. Strong and G. F. Saunders. "Positional cloning and characterization of a paired box- and homeobox-containing gene from the aniridia region." Cell. 67: 1059-1074, 1991.
- 57. Treisman, J., E. Harris and C. Desplan. "The paired box encodes a second DNA-binding domain in the paired homeo domain protein." Genes & Dev. 5: 594-604, 1991.
- 58. Waardenburg, P. J. "A new syndrome combining developmental anomalies of the eyelids, eyebrows and nose root with pigmentary defects of the iris and head hair with congenital deafness." Am. J. Hum. Genet. 3: 195-253, 1951.
- 59. Wang, L.-M., D. K. Weber, T. Johnson and A. Y. Sakaguchi. "Supercoil sequencing using unpurified templates produced by rapid boiling." BioTechniques. 6(9): 839-843, 1988.
- 60. Weber, J. L., A. E. Kwitek and P. E. May. "Dinucleotide repeat polymorphisms at the D11s419 and CD3D loci." Nucleic Acids Res. **18**(13): 4036, 1990.
- 61. Webster, W. "Embryogenesis of the enteric ganglia in normal mice and in mice that develop congenital aganglionic megacolon." J. Embryol. Exp. Morphol. 30: 573-585, 1973.
- 62. Wilcox, E. R., N. M. Rivolta, B. Ploplis, S. B. Potterf and J. Fex. "The HuP2 gene is mapped to chromosome 2, together with a highly informative CA dinucleotide repeat." Hum. Molec. Genet. 1: 215, 1992.

